Electrical Modeling of Excitable Cells

Asif Mehmood

December 23, 2013

Contents

List of Figures

List of Tables

Abstract

The human brain is the most wonderful and mysterious organ of human body. This masterpiece creation of nature manages the actions in such a way that they happens in real time at right place. It also stores information so that the behavior can be modified according to the past experience. A single cubic centimeter of human brain contain several million nerve cells, each of which may communicate with thousands of other cells in information processing networks that make the most elaborate computer look primitive. These cells can be excited by stimulation, therefore are known as excitable cells. The excitable cells found in brain are called neurons. Neuron is the basic structural and functional unit of human brain which is specialized for the conduction of nerve impulses. Upon receiving a threshold stimulus, the membrane of neuron quickly depolarizes at the point of stimulation, and this electrical impulse propagates along the axon of neuron in the form of action potential. Hodgkin and Huxley model explains in detail the formation and propagation of action potential through nerve cell. This model contains the set of non-linear differential equations that can be solved by numerical method techniques only. Computationally the model is very complex and almost takes 1200 flops for simulating a single neuron. Another category of excitable cells are found in heart, called cardiac myocytes. The formation of action potential of cardiac myocytes can be explained by Luo-Rudy model which is the extension of Hodgkin and Huxley model. Computationally Luo-Rudy model is almost ten times more complex than Hodgkin and Huxley model. Therefore, there is a need of simpler model for excitable cells that can implement the behavior of excitable cells down to ionic channel level. In our study we used a new concept of actifiers for the first time to model excitable cells. Actifiers are the electrical circuits that can amplify and rectify at the same time. The model is conductance based and captures the ionic channel level characteristics of excitable cells. Computationally, the actifier model takes 12 flops for simulating neuron and 15 flops for simulating cardiac myocyte, almost a decrease of 100 times in computational cost of Hodgkin and Huxley model. We reported some common behaviors of neurons and cardiac myocytes. The results are in good agreement with the experimental data.

Declaration

No portion of the work referred to in this thesis has been submitted in support of an application for another degree or qualification of this or any other university or other institute of learning.

Acknowledgement

I would like to express my thanks and sincere gratitude to my advisor **Dr. Jamil Ahmad**, Head Of Department, RCMS, NUST, for his continuous support, helpful advice and valuable guidance throughout this project work. His emphasis for excellence kept me well-directed and focused. He has made me able to follow the thesis plan very smoothly through his well defined execution and cooperation day in and day out. His cheerful and enthusiastic encouragement was a source of strength for me to complete this project.
I am immensely grateful to **Dr. Muhammad Mukaram Khan**, Assistant Professor, RCMS, NUST, for giving me valuable inputs. His vast experience of the field has assisted me in a very sophisticated manner right to the completion.
I am thankful to **Dr. Meraj Mustafa Hashmi**, Assistant Professor, RCMS, NUST, for his support i mathematical problems.
My sincere appreciation goes to **Engineer Sikandar Hayat Mirza**, Assistant Professor, RCMS, NUST, for providing the necessary resources and facilities to carry out this project in time.
My sincere gratitude is to **Dr. Touqeer Ahmed**, Assistant Professor, ASAB, NUST, whose emphasis for excellence kept me focused on to my project and helped me complete it in time. I thank him for providing the necessary resources and facilities to carry out this project in time.
I would also acknowledge the active support, I got from all my class fellows, especially, Azmat Ali Khan and other departmental seniors, especially, Saba Munawar, Zurah Abbasi and Noreen Akhtar for providing the necessary resources and facilities to carry out this project in time.
Finally, I am extremely gratified and indebted to my family members for their enormous support, persistent encouragement and earnest prayers throughout this project.

Copyright

Part I

Neuron

Chapter 1

Introduction

The human brain is the most complex structure that can be regarded as the measure of complexity of the known universe. This complex structure is composed of excitable cells called neurons. All neurons transmit information in the form of impulses [9, 17]. When a neuron is in its equilibrium state, its membrane has an electrical potential of approximately -70 millivolts, that is, the inside of the membrane has more negative ions than the outside. Neuron membrane is made of phosphoric acid and fatty acid and contains some negatively charged protein molecules scattered throughout it [46, 27]. These protein molecules are the chemical receptors of particular ions and are called ion channels. The ion channels allow specific type of ions to pass through the membrane of the cell. For example, the ion channels that only allow the sodium ions to pass through the membrane are called sodium ion channels [6, 28]. These ion channels are voltage sensitive gates and are opened at particular voltage level. Similarly the closing of ion channel gates also occurs at particular potential difference. For example, sodium gates open at -30 millivolts and close at +35 millivolts [50].

The concentration of sodium and potassium ions is not same inside and outside the cell. This difference in ionic concentration causes a concentration gradient across the neuron membrane. Initially the concentration of potassium ions is much higher inside the neuron than the fluid outside the cell [19, 11]. There are leakage channels that allows the potassium ions from inside the neuron to move outside, to balance its concentration under a diffusion force caused by the concentration gradient. The diffusion process leaves an excess of negative charge inside the cell body which causes a strong potential difference across the cell membrane [25]. Due to this potential difference, an electric force develops in the opposite direction to the diffusion force and tries to stop the potassium ions flow. When these two forces balance each other, the further movement of potassium ions is stopped from inside to the outside of the cell [11, 53, 30].

Under equilibrium state, the concentration of potassium ions inside the cell is 400 millimole per liter and 20 millimole per liter outside the cell. Due to the movement of potassium ions outside the cell a negative potential appears across the membrane [6]. The membrane at equilibrium is slightly permeable to sodium ions due to leakage channels. When chemical substance called neurotransmitter is released, it moves the potential difference of membrane in a positive direction and activates the cell membrane by developing an action potential across the membrane. This action potential propagates in the form of

electrical impulse through the axon [56, 32].
In 1952, Hodgkin and Huxley developed a conductance based model to explain the generation and propagation of action potential through the axon of giant squid [20, 33]. Their model gives good approximation about how the membrane behaves when ions are exchanged. The Hodgkin and Huxley model contains set of non-linear differential equations that makes the model very complex. Other simple models of neuron are integrate and fire model and Izhikevich model [15]. These models are very efficient computationally but are not able to implement the actual conductance based behavior of the neuron.
The cells in heart are also excitable cells called cardiac myocytes. The cardiac myocytes also generates action potential like neurons but their action potential is due to excitation contraction process. The function of ion channels in myocytes is similar to that of neurons, however, their action potential is due to the mechanical impulses of excitation contraction process [16, 10]. Based on Hodgkin and Huxley model, a model is developed for cardiac myocytes called Luo-Rudy dynamic model. This model is also very complex like Hodgkin and Huxley model. These two models are very accurate at single cell level but are complicated when we want to simulate the population of excitable cells [7]. Therefore, we need a simple model that can represent the excitable cells and all of its behaviors by slight modifications.
In our study we tried to develop a unified model for excitable cells that can represent the generation of action potential in both type of cells.

1.1 Neuron

A neuron is the basic building block of the nervous system that is responsible for communicating information in both chemical and electrical forms. There are several different types of neurons responsible for different tasks in the human body. Sensory or afferent neuron carries massage from a sense organ to the brain. Motor or efferent neuron transmit information from the brain to the muscles of the body. Interneurons or associative neuron are responsible for communicating information between different neurons in the body. A neuron has three main parts; membrane, axon and dendrite.

1.1.1 Membrane

The membrane of neuron is made of phosphoric acid and fatty acid having thickness of about $3-4$ nanometers. It keeps the neuron in contact with the ionic solution around it containing sodium, potassium, calcium and chloride ions. The membrane is partially permeable and contains negatively charged protein molecules scattered throughout it. Due to the presence of positive and negative charges, it behaves like capacitor. The protein molecules acts as chemical receptors for particular ions and therefore, these protein molecules are called ionic channels. For example, the protein molecules that only allow the movement of sodium ions are called sodium channels. These channels requires certain potential difference for their activation. For sodium channels the value of this potential is about -30 millivolts. Similarly, for potassium ions, the value of activation channel

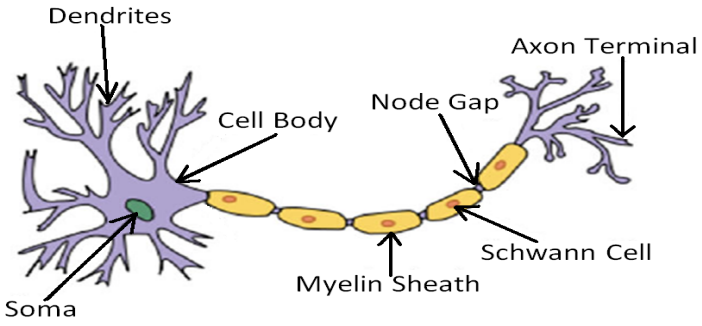

Figure 1.1: Anatomy of Neuron [28]

potential is +35 millivolts. The closing of ionic channels is also the function of potential difference. Some channels called leakage channels, remain open for the free movement of ions through the membrane.

1.1.2 Axon

The long wire like structure that acts as output terminal of neuron is called axon. The axon may branch and send multiple fibres to attach to the other neurons. These fibers are called axon terminals. The axon contains small tubes that carries chemical substances. These tubes are called micro-tubules. The chemical substances carried by micro-tubules are called neurotransmitters. The larger axons are covered with a layer of fatty insulation called myelin sheath. Therefore, axon transports the neurotransmitters produced in the cell body to the target neuron. The target neuron is also called postsynaptic neuron. The axon terminals contains a large number of chemical pockets which stores neurotransmitters. These pockets are called vesicles.

1.1.3 Dendrite

The cell body of the neuron contains multiple fibres called dendrites. The dendrites of a neuron may range from a few short fibres to a huge mass of entangled bushes. A typical neuron can have 10,000 to 100,000 dendrites. The axons from one neuron can be connected to the cell body of another neuron directly or through dendrites. The dendrites of many neurons contains thousands of little extensions called dendritic spines.

1.1.4 Synapse

The point of functional contact between two neurons is called synapse. In between the contact points, there is a space of about 20 nanometers called synaptic cleft. When a synapse is active, the vesicles open and release neurotransmitters into the synaptic cleft. The synapse can be either excitatory or inhibitory depending upon the type of neurotransmitter. The excitatory synapses increase the activation of target neurons while the inhibitory synapse reduce their activation.

1.1.5 Action Potential

The waveform of potential across the membrane of neuron due to the ion distribution is called membrane potential or action potential. The formation of action potential is due to the diffusion force and electric force. Diffusion force is generated due to the difference in ionic concentration inside and outside the cell, while electric force arises due to electrostatic force of attraction between positive ions and negatively charged protein molecules. The concentration of ions inside and outside the neuron is not same. Due to this concentration difference, a concentration gradient force is established across the membrane. This force is called diffusion force. The concentration of potassium ions is usually much higher inside the neuron than the fluid outside the cell. The leakage channels allow the potassium ions to move outside the cell to balance the concentration gradient under the action of diffusion force. The neuron contains negatively charged protein molecules which always remain inside the cell due to their larger size. Therefore, diffusion force leaves a negative charge inside the neuron and net positive charge outside the cell. Due to these opposite charges, a strong electric force appears across the membrane. The direction of this electric force is opposite to the diffusion force, therefore, electric force tends to stop the outward flow of potassium ions from the membrane. When electric force becomes equal to the diffusion force, an equilibrium is established across the cell membrane and further movement of potassium ions is stopped. The equilibrium state is achieved when the concentration of potassium ions inside the cell is 400 millimole per liter and 20 millimole per liter outside the cell. The resting membrane potential due to potassium ions can be calculated by using Nernst equation;

$$V = \frac{RT}{kF} log \frac{[I^+]_{out}}{[I^+]_{in}}$$

Where k, R and F are constants, T is absolute temperature and $[I^+]$ is the concentration of positive ions. At normal temperature of 18^0C;

$$\frac{RT}{kF} = 58$$

Therefore, Nernst equation gives the resting potential of potassium ions as;

$$V = 58log\left[\frac{20}{400}\right] = -75.46mV \approx -75mV$$

The Nernst equation can be extended to take into account the effect of sodium, calcium and chloride ions concentrations. Thus the resting potential of neuron is the sum of resting potentials contributed by all the ionic channels. The typical value of neuron resting potential is about -65 millivolts.

The membrane at resting state is slightly permeable to sodium ions due to leakage channels. When a large quantity of neurotransmitter is released by the presynaptic neuron, it can trigger a stronger response in the membrane potential of postsynaptic neuron. If the neurotransmitter is excitatory, it will move the potential difference in a positive direction from -65 millivolts to -30 millivolts called threshold potential. As -30 millivolts is the activation potential for sodium channels, therefore, this threshold potential will open all sodium channels so that sodium ions can easily move inside the cell. The concentration of sodium ions outside the cell is greater, therefore, diffusion force pushes the sodium ions inside the cell. As inside the cell there are negatively charged protein ions that tends to attract positively charged sodium ions, thus, positively charged sodium ions rush inside the cell due to electrical force. Due to same direction of diffusion and electrical force on sodium ions, the movement of sodium ions inside the cell body is 500 times more than in the resting state. This rapid inward movement of sodium ions again develops the equilibrium condition when membrane potential reaches the value of +50 millivolts. At this potential all sodium channels are closed and potassium channels are activated. The opening of potassium channels let the potassium ions to move outside the cell and potential of membrane goes towards negative side from +50 millivolts to -65 millivolts. The opening and closing of potassium ion channels is much slower than sodium ion gates, as a result membrane potential goes more negative towards -75 millivolts. This state of more negative voltage than the resting potential (-65 millivolts) is called hyperpolarization. The few voltage dependent gates of potassium ions are closed in hyperpolarization state and the membrane potential returns back to the normal resting voltage of -65 millivolts. During this time when membrane potential tends to move towards -65 millivolts, neuron can not be electrically stimulated to generate another action potential. This time interval in which neuron can not generate action potential is called absolute refractory period. The action potential of typical neuron is shown in the figure 1.2.

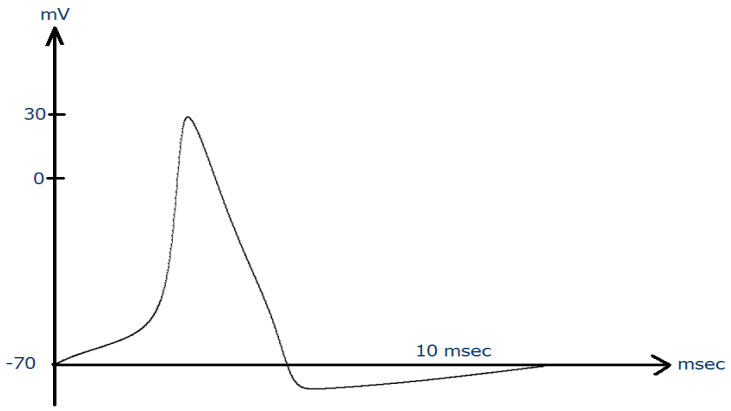

Figure 1.2: Action potential of neuron [26]

1.2 Neuron Models

Many attempts were made to explain the generation and propagation of action potential through the nerve cells. Some most widely accepted models of neuron are described below.

1.2.1 Leaky Integrate and Fire Model

The simplified model of neuron is called Leaky Integrate and Fire (LIF) model. This model is the parallel combination of a capacitor C and resistor R. The source of current $I(t)$ generates a pulse and capacitor is charged through resistor R. The circuit of LIF model is shown in figure 1.3. Applying Kirchhoff's current law, the external current $I(t)$

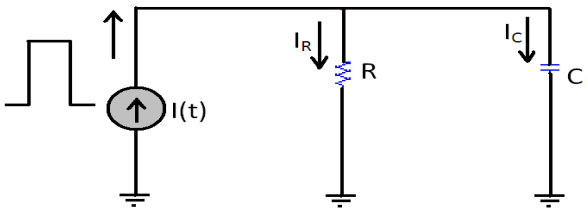

Figure 1.3: Leaky Integrate and Fire Model

is the sum of current through resistor R and capacitor C. Mathematically;

$$I(t) = I_R + I_C$$

From basic circuit theory, we can write the current I_R and I_C, when voltage across resistor and capacitor is given by v;

$$I_R = \frac{v}{R}$$

$$I_C = C\frac{dv}{dt}$$

Therefore, the total current $I(t)$ can be expressed as;

$$I(t) = \frac{v}{R} + C\frac{dv}{dt}$$

By simplification, we get the equation for LIF model as;

$$\tau\frac{dv}{dt} + v(t) = RI(t) \quad ; \quad \tau = RC$$

Let the circuit is stimulated by a constant input current I_o, in this case the solution of circuit can be expressed as;

$$v(t) = RI_o(1 - e^{-\frac{t}{\tau}})$$

LIF model takes approximately 5 flops to simulate a single neuron and can implement some common behaviors of neuron like tonic spiking and class-I excitability [21].

1.2.2 Hodgkin and Huxley Model

Hodgkin and Huxley developed a mathematical model to explain the behavior of nerve cells in a giant squid in 1952. This model is the most accepted one to capture neural dynamics in biological neurons in the form of action potential (figure 1.4). Hodgkin and Huxley explained the formation of action potential on the basis of ionic channels. According to this model, there are three types of channels contribute to the changes in the membrane potential:
1) leakage channels
2) voltage dependent potassium channels
3) voltage dependent sodium channels
The voltage controlled channels have varying conductances which are dependent on the

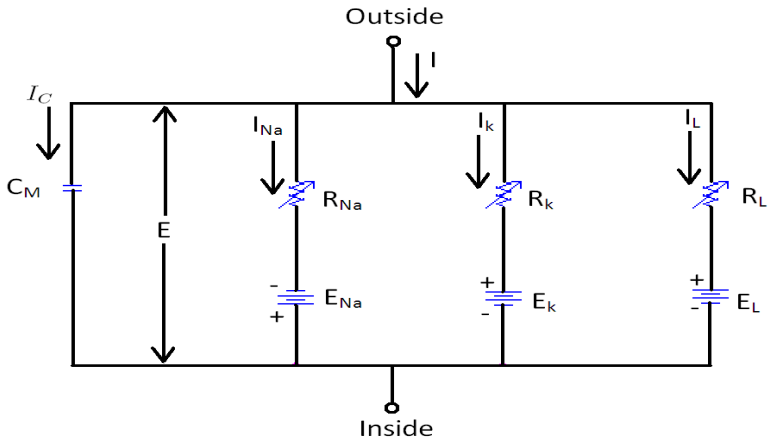

Figure 1.4: Hodgkin and Huxley Model

number of channels opened at a particular time. Hodgkin and Huxley devised an empirical formula to these channels which they found from their experiments. They defined the conductances of these channels using three variables n, m and h, chosen appropriately to approximate their behavior to the experimental data. The variables n, m and h describe the activation of potassium ionic channels, sodium ionic channels and the inactivation of sodium ionic channels respectively. The effect of these variables on the channel conductance is given by;

$$g_k = \bar{g_k} n^4$$

Where $\bar{g_k}$ is a constant, and n is a dimensionless variable that varies from 0 to 1. It is the proportion of ionic channels that are open. These variables represent the number of activation or inactivation gates such as the voltage-gated K^{+1} current with four activation gates (represented as n^4), and the voltage-gated Na^{+1} current with three activation gates (m^3) and one inactivation gate (h^1). The variable n can be defined by the equation:

$$\frac{dn}{dt} = \alpha_n(1-n) - \beta_n n$$

where α_n is the rate of closing of the channels and β_n is the rate of opening. Together, these variables represent the total rate of change in the channels during an action potential. The sodium conductance can be described by the equation;

$$g_{Na} = m^3 h \bar{g_{Na}}$$

Where $\bar{g_{Na}}$ is a constant, m is the proportion of activation ionic channels and h is the proportion of inactivation of ionic channels. Let the variable x represents n, m and h, we can write a generalized equation as;

$$\frac{dx}{dt} = \alpha_x(1-x) - \beta_x x$$

Where x is either m, n or h, α and β are the rate of closing and opening of the channels. Together, these variables represent the total rate of change in the channels during an action potential. Hodgkin and Huxley selected these variables to get a reasonable fit to the experimental data.
Applying Kirchoff's current law on figure 1.4, we can write:

$$I = I_C + I_{Na} + I_K + I_L$$

$$I_C = C\frac{dV}{dt}$$

$$I_{Na} = g_{Na}(E - E_{Na})$$

$$I_K = g_k(E - E_K)$$

$$I_L = g_L(E - E_L)$$

$$I(t) = C\frac{dV}{dt} + g_{Na}(E - E_{Na}) + g_k(E - E_K) + g_L(E - E_L)$$

$$\frac{dV}{dt} = \frac{1}{C}[I(t) - g_{Na}(E - E_{Na}) - g_k(E - E_K) - g(E - E_L)] \tag{1.1}$$

Above equation (1.1) is called the Hodgkin and Huxley model. Computationally, Hodgkin and Huxley model takes 1200 flops to simulate a single neuron. The computational cost of model is the measure of accuracy in this case.

1.2.3 Izhikevich Model

Leaky integrate and fire model is the most simplest model of spiking neurons while Hodgkin and Huxley model is the most complex one based on the actual conductance based behavior of spiking neuron. In 2003, Eugene Izhikevich proposed a simplified model for spiking neurons based on leaky integrate and fire model. This model is called quadratic

integrate and fire model or Izhikevich model. Izhikevich model is based on the behavior prediction technique without knowing the deep understanding of the neuron and ionic channels. Computationally, Izhikevich model is simpler like leaky integrate and fire model but efficient like Hodgkin and Huxley model. The only drawback in Izhikevich model is, it is not conductance based model. This model can be used only for simulation purposes without knowing the actual dynamics of the neuron. Izhikevich model can be expressed mathematically as;

$$\frac{dv}{dt} = 0.04v^2 + 5v + 140 - u + I$$

$$\frac{du}{dt} = a(bv - u)$$

Here v and u represents membrane potential and membrane recovery for the activation of K^{+1} ionic currents and inactivation of Na^{+1} ionic currents, and it provides negative feedback to v. The variables and parameters in the model are all dimensionless values that can be thought of as representing various states or properties of the neuron. In these equations,
v is membrane potential
u is membrane recovery
a is the time scale of u
b relates subthreshold sensitivity of u to v
After the spike reaches its threshold value (+30 millivolts), the membrane voltage and the recovery variable are reset according to the model. Izhikevich model can be plotted (figure 1.5) for regular spiking in MATLAB code given below.

```
C=100; vr=-60; vt=-40; k=0.7; % parameters used for RS
a=0.03; b=-2; c=-50; d=100; % neocortical pyramidal neurons
vpeak=35; % spike cutoff
T=1000; tau=1; % time span and step (ms)
n=round(T/tau); % number of simulation steps
v=vr*ones(1,n); u=0*v; % initial values
I=[zeros(1,0.1*n),70*ones(1,0.9*n)];% pulse of input DC current
for i=1:n-1 % forward Euler method
v(i+1)=v(i)+tau*(k*(v(i)-vr)*(v(i)-vt)-u(i)+I(i))/C;
u(i+1)=u(i)+tau*a*(b*(v(i)-vr)-u(i));
if v(i+1)>=vpeak % a spike is fired!
v(i)=vpeak; % padding the spike amplitude
v(i+1)=c; % membrane voltage reset
u(i+1)=u(i+1)+d; % recovery variable update
end;
end;
plot(tau*(1:n), v); % plot the result
```

Izhikevich model displays almost all possible behaviors of excitatory cortical neurons such as Regular Spiking, Intrinsically bursting and Chattering etc. The model also displays all possible inhibitory cortical cell's responses such as Fast Spiking and Low threshold spiking. The model also can successfully exhibit the behavior of thalamo cortical neurons. On October 27, 2005 Izhikevich simulated a neural network that had the size of the human brain (10^{11} *neurons*) using his neural network model. Therefore, we can say that the most

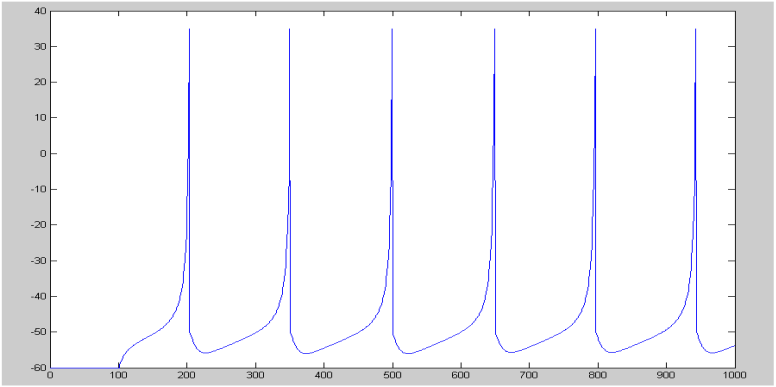

Figure 1.5: MATLAB simulation of Izhikevich model for regular spiking

efficient computational model is, Izhikevich model.

1.2.4 Comparison

A brief comparison of neuron models is presented in table-I which compares the complexity of neuron models in number of flops.

Table 1.1: This table compares all the well known models of neurons with AJ model. BM stands for Biophysically Meaningful, M stands for myocyte and other column headings are stated in the result section.

Models	BM	TS	PS	TB	PB	MM	SFA	C-1	C-2	SL	SO	R	I	RS	RB	TV	B	DAP	A	IIS	IIB	C	M	FLOPS
Integrate and Fire	-	+	-	-	-	-	-	+	-	-	-	-	+	-	-	-	-	-	-	-	-	-	-	5
Integrate and Fire with adapt.	-	+	-	-	-	-	+	+	-	-	-	-	+	-	-	-	-	+	-	-	-	-	-	10
Integrate and Fire or burst	-	+	+	-	+	-	+	+	-	-	-	-	+	+	+	-	+	+	-	-	-	-	-	13
Resonate and Fire	-	+	+	-	-	-	-	+	+	-	+	+	+	+	-	-	+	+	+	-	-	+	-	10
Quadratic Integrate and Fire	-	+	-	-	-	-	-	+	-	+	-	-	+	-	-	+	+	-	-	-	-	-	-	7
Izhikevich (2003)	-	+	+	+	+	+	+	+	+	+	+	+	+	+	+	+	+	+	+	+	+	+	-	13
FitzHugh Nagumo	-	+	+	-		-	-	+	-	+	+	+	-	-	-	+	+	-	+	+	-	-	-	72
Hindmarsh Rose	-	+	+	+			+	+	+	+	+	+	+	+	+	+	+	+	+	+		+	-	120
Morris lecar	+	+	+	-		-	-	+	+	+	+	+	+	-	-	+	+	-	+	+	-	-	-	600
Wilson	-	+	+	+			+	+	+	+	+	+	+	-	+	+	-	+	+				-	180
Hodgkin Huxley	+	+	+	+			+	+	+	+	+	+	+	+	+	+	+	+	+	+		+	-	1200

Chapter 2

Methodology

The excitable cells can be modeled by active circuit elements like transistors or operational amplifier due to the amplified form of action potential generated by small input stimulus. We modeled the excitable cells with active circuit element operational amplifier due to its wide range of operations and other passive elements like capacitor, resistors and p-n junction diodes. A brief description of each circuit element is given below:

2.1 Operational Amplifier

An amplifier that can perform mathematical operations such as addition, multiplication, integration and differentiation etc is called operational amplifier. It is used widely as high voltage gain amplifier and as a switch. Symbolically operational amplifier is shown in figure 2.1. The operational amplifier has two inputs and one output. One is known as

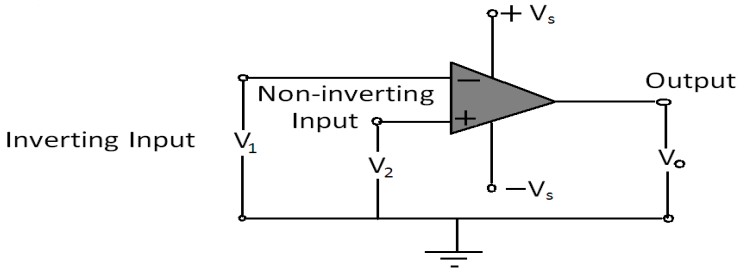

Figure 2.1: Schematic diagram of operational amplifier

the non-inverting input (+) and the other as inverting input (-). It is usually energized from a dual balanced D.C. power supply giving equal positive and negative voltages in the range $\pm 5V$ to $\pm 15V$. The center point of the power supply (i.e. 0V) is common to the input and output circuits and is taken as their voltage reference level.

Figure 2.2 shows a simplified circuit of a non-inverting operational amplifier. The input

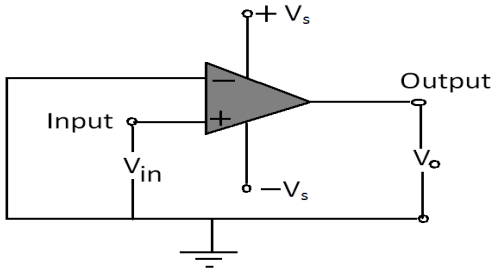

Figure 2.2: Schematic diagram of operational amplifier in non-inverting mode

voltage is connected to the non-inverting (+) input and earth or ground voltage 0V. The inverting input (-) is connected to earth, and the output voltage V_o is between the output terminal and earth. The operational amplifier now acts as a non-inverting voltage amplifier. This means that the output is the exact amplified copy of the input.

The non-inverting operational amplifier with feedback is shown in figure 2.3. In this case the input voltage V_{in} is applied to the non-inverting (+) terminal of operational amplifier. The resistance R_i is called input resistance and resistance R_f is called feedback resistance. The transfer function of operational amplifier in non-inverting mode is given in equation (2.1).

$$\frac{V_{out}}{V_{in}} = 1 + \frac{R_f}{R_i} \tag{2.1}$$

Equation (2.1) shows that the gain of amplifier depends upon the externally connected resistances R_i and R_f. The positive sign of gain indicates that the input and output signals are in phase.

2.2 Linear Resistor

Resistor is a device that limits the electric current in a circuit. Resistance of a resistor is denoted by R and it is the measure of the opposition to the motion of charge carriers. In metallic conductors the charge carriers are the free electrons and their motion is opposed

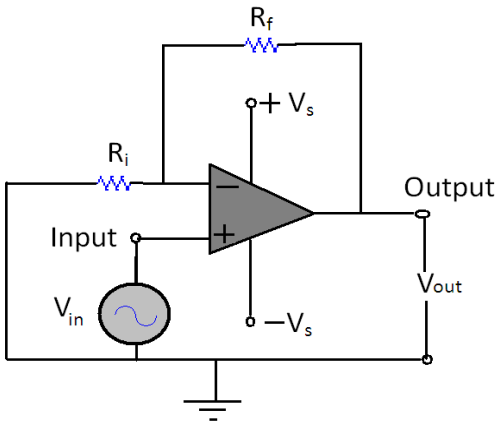

Figure 2.3: Schematic diagram of operational amplifier in non-inverting mode with feedback resistance

due to their continuous collisions with the lattice atoms of the solid conductors. The value of resistance R depends on the nature, dimensions and the physical state of the conductor. It is observed experimentally that at constant temperature the resistance of a conductor is directly proportional to length L and inversely proportional to cross-sectional area A. Mathematically we can write,

$$R \propto \frac{L}{A}$$

$$R = \rho \frac{L}{A} \tag{2.2}$$

Where ρ is the constant of proportionality and is called the resistivity or specific resistance of the material. A wire with small length and greater cross-sectional area will offer less resistance. To explain this concept, we consider a hollow cylinder with length L and inner and outer radii r_1 and r_2, made of a material with resistivity ρ. Let a potential difference is created between the inner and outer surfaces of the cylinder so that current flows radially through the cylinder as shown in figure 2.4. We assumed that the current is flowing in radial direction towards the outside, not along the length of the conductor. As charge travels in the radial direction, the cross-sectional area of cylinder varies from $2\pi r_1 L$ to $2\pi r_2 L$, from inner surface to the outer surface. In this situation, equation (2.2) cannot be applicable directly. Let the length of current path in radial direction be dr and the corresponding resistance of this shell be dR. In this case, equation (2.2) can be written as;

$$dR = \frac{\rho dr}{2\pi r L}$$

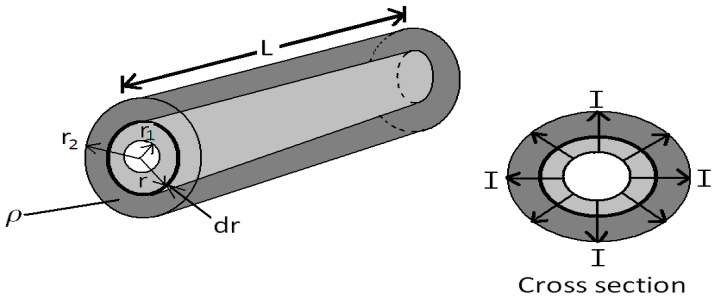

Figure 2.4: Resistance of cylinder due to radial current flow

Integrating left hand side over R and right hand side from r_1 to r_2;

$$\int dR = \frac{\rho}{2\pi L} \int_{r_1}^{r_2} \frac{dr}{r}$$

$$R = \frac{\rho}{2\pi L} ln \frac{r_2}{r_1}$$

We can observe that, the resistance strongly depends upon the geometry of the conductor. The neurons in our body can be considered as cylinder due to the long extension of axon. The axon has cylindrical membrane similar to the resistor shown in figure 2.4, having one conducting fluid inside the membrane and other outside it. In equilibrium state, all the inner fluid is at the same potential, so no current can flow along the length of the axon. If axon is stimulated, the charged ions flow radially across the cylinder membrane at the point of stimulation. This flow creates a potential difference across the membrane at the point of stimulation and propagates along the length of axon in the form of action potential.
The resistance of the neuron is usually described by another parameter called conductance, denoted by g. The conductance of a material is the reciprocal of resistance. Mathematically, we can write;

$$g = \frac{1}{R}$$

The resistance of material also depends upon temperature. It is found experimentally that with increase in temperature, resistance of conductor increases but in case of semiconductors and insulators, resistance decreases with increasing temperature. The increase in resistance $\triangle R$ for conductors is directly proportional to original resistance R_o at zero degree centigrade and rise in temperature $\triangle T$. Mathematically, we can write;

$$\triangle R \propto R_o \triangle T$$

$$\triangle R = \alpha R_o \triangle T$$

Where α is the constant of proportionality and is called temperature coefficient of resistance. Let the resistance of material at 0^oC is R_o and at T^oC is R_T, the increase in resistance $\triangle R$, can be expressed as;

$$\triangle R = R_T - R_o$$

Therefore, at particular temperature T^oC resistance can be written as;

$$R_T - R_o = \alpha R_o \triangle T$$

$$R_T = R_o + \alpha R_o \triangle T$$

The resistance of material that changes with temperature is called non-linear resistance. If temperature is kept constant, the resistance variation becomes zero. In this case resistance will be linear and Ohm's law is applicable for such resistance. The characteristic equation of linear resistor can be defined by Ohm's law as;

$$v = iR \tag{2.3}$$

Equation (2.3) is valid only for linear operation of resistance when resistance remains constant. In human body temperature remains constant (37^oC) for normal person, therefore, for neurons we can describe the current voltage characteristics by applying Ohm's law. We can find the typical value of resistance for neuron by assuming that temperature of neuron remains constant when it fires action potential pulse. In this case resistance only depends upon surface area of neuron that contributes in the formation of action potential. The resistance of a typical patch of membrane is,

$$R_M = 10,000 \Omega cm^2$$

The total resistance of neuron with radius r is given by;

$$R_m = \frac{R_M}{4\pi r^2}$$

Substituting the appropriate values we have;

$$R_m = \frac{10,000 \Omega cm^2}{4\pi \times (20 \times 10^{-4} cm)^2} = 198 M\Omega$$

The high resistance of neuron does not allow the movement of ions in equilibrium state.

2.3 Capacitor

Capacitor is a device which stores charge in its electric field. A typical capacitor consists of two parallel conducting plates placed close to each other. The space between the plates may be filled with a dielectric material such as air, mica or paraffin. Charging of capacitor is usually accomplished by transferring the charge from one plate to the other by means of a battery. The charge gained by one plate is equal to the charge lost by other plate, that is, the net charge is zero on the capacitor. However, when we say that the charge of a capacitor is Q, it means that one plate has charge $+Q$ while the other has charge $-Q$. The capability of a capacitor to store charge is called capacitance. The charge Q, which resides on one of the plates, depends upon the potential difference between the plates.

The larger the voltage of the battery, the greater will be the charge on the capacitor. If v is the potential difference across the plates, then

$$Q \propto v \quad or \quad Q \; = \; Cv$$

Differentiating with respect to t we get,

$$\tfrac{dQ}{dt} = C\tfrac{dv}{dt}$$

By definition,

$$i = \tfrac{dQ}{dt}$$

Therefore, the characteristic equation of capacitor can be written in the form of equation (2.4), given below;

$$i = c\frac{dv}{dt} \tag{2.4}$$

From equation (2.4) we can conclude that, the circuit consists of capacitor can be considered as differentiator. The opposition offered by capacitor in time varying source is called capacitive reactance, denoted by X_c. The capacitive reactance X_c is inversely proportional to capacitance and frequency of time varying signal applied at capacitor. Mathematically, we can write,

$$X_c \propto \tfrac{1}{fC}$$

$$X_c = \tfrac{1}{2\pi fC}$$

When direct current signal (f=0) is applied on capacitor, we see that capacitive reactance X_c becomes infinite, representing short circuit. Therefore, capacitor behaves as short circuit for direct current source. If the frequency of applied signal increases, capacitive reactance X_c decreases. At high frequencies capacitive reactance becomes very low and capacitor behaves as short circuit.
The cell body of neuron can be assumed as spherical capacitor with non-uniform radius. The capacitance of spherical capacitor with inner radius r_1 and outer radius r_2 can be expressed as;

$$C = 4\pi\epsilon_o\frac{r_1 r_2}{r_2 - r_1} \tag{2.5}$$

The cell body of neuron can store electrical charge in the form of ions. For simplicity we assume that the cell body of neuron is uniform sphere of radius r and charge is evenly distributed throughout the cell body. In this case, we can define the effective area of spherical surface that stores charge and separation between the surfaces as;

$$A = r_1 r_2$$

$$d = r_2 - r_1$$

Therefore, equation (2.5) can be written as;

$$C = 4\pi\epsilon_o\frac{A}{d} \tag{2.6}$$

Let C_m be the capacitance of spherical shell of radius r, it can be shown that the capacitance of spherical shell can be written as;

$$C_m = 4\pi r^2 C_M$$

where C_M is constant and is called membrane capacitance per unit area. Its typical value is given by;

$$C_M = 4\pi\epsilon_o \tfrac{1}{d} = 1\mu F/cm^2$$

Since for neurons $r = 20\ microns$, so we have;

$$C_m = 4\pi \times 1\mu F/cm^2 \times (20 \times 10^{-4} cm)^2 = 5 \times 10^{-11} F$$

$$C_m = 50pF$$

Also the resistance of neuron is;

$$R_m = 198M\Omega$$

Depending upon the values of capacitance and resistance we can define the membrane time constant τ_m as;

$$\tau_m = R_m C_m = \tfrac{R_M}{4\pi r^2} \times 4\pi r^2 C_M$$

$$\tau_m = R_M C_M = 1\mu F/cm^2 \times 10,000\Omega cm^2 = 10\ msec$$

Therefore, we can assume the values of capacitance and resistance for neuron as, $C = 50pF$, $R_K = 198M\Omega$ and $R_{Na} = 65M\Omega$, where R_K is the resistance of potassium ion channels and R_K is the resistance of sodium ion channels. The value of R_{Na} is taken three times less than that of R_K because sodium ion moves much faster than potassium ions [20, 49].

2.4 P-N Junction Diode

P-N junction diode is a semiconductor device that allows the electric current to flow in one direction only. When a p-type semiconductor is joined or doped to an n-type semiconductor, the region arises where both materials are joined, is called a $p-n$ junction. The junction is not formed by simply placing the two materials in contact with each other, but rather through a fabrication process that creates a transition from p-type to n-type material within a single crystal. Before doping, both type of materials are electrically neutral. The reason is that each acceptor atom A and each donor atom D has the same number of electrons as protons. However, there is a greater concentration of electrons in the n-region as compared with their concentration in the p-region. Likewise, there is higher concentration of holes in the p-region as compared with the n-region. Due to concentration difference between charge carriers, a diffusion force is established across the junction that tends to push the charge carriers in opposite directions. Therefore, at the instant the p-type and n-type materials are joined, electrons near the junction diffuse from the n-region into the p-region as shown in figure 2.5. For each electron that leaves the n-region to cross the junction into p-region, a donor atom that now has a net positive charge is left behind. Similarly, for each hole in the p-region that receive an electron from the n-region, an acceptor atom acquires a net negative charge. The result of this process

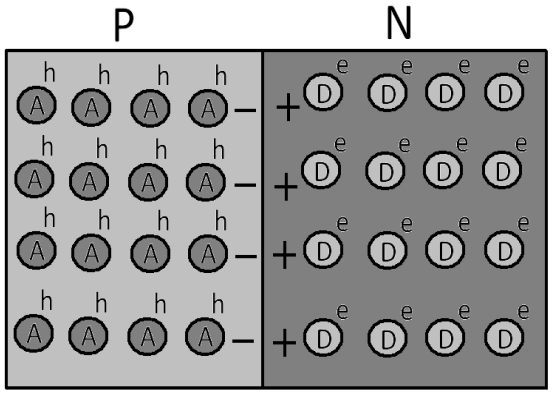

Figure 2.5: The $p-n$ junction showing charged ions after holes and electrons diffusion. D=donor atom; A=acceptor atom; e=associated electron; h=associated hole; + = positively charged ion; - = negatively charged ion.

is that positively charged donor ions accumulate just inside the n-region and negatively charged acceptor ions accumulate just inside the p-region. This charge distribution is shown in figure 2.5.
The accumulation of charge of opposite polarities in the two separated regions give rise to a potential difference and electric field across the junction region. The direction of electric field is such that it opposes the flow of electrons from the n-region into the p-region. Therefore, after the initial surge of charge across the junction, the diffusion current dwindles to a negligible amount. The region of junction is populated by uncovered positive and negative ions. There are no mobile charge carriers in this region. The n-region electrons have migrated to the p-side and have filled the p-region holes. Because all charge carriers have been depleted from this region, it is called depletion region. It is also called the barrier region because the potential difference that exists across the junction due to the oppositely charged sides of the junction acts as a barrier to further diffusion current. The width of depletion region depends on how heavily the p and n materials have been doped. Symbolically, $p-n$ junction is represented by an arrow head and a line in front of it. The arrow head represents p-type material and line in front of it represents n-type material as shown in figure 2.6. There are two schemes of connecting $p-n$ junction with battery:

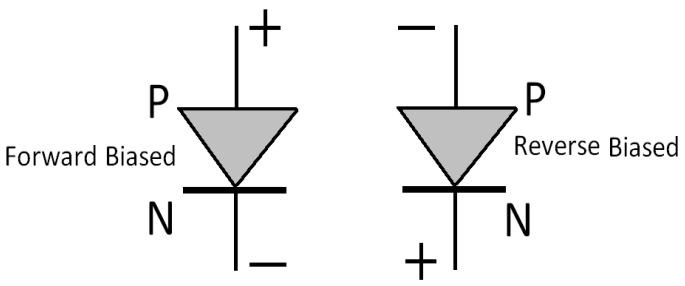

Figure 2.6: Biasing of $p-n$ junction; + = positive terminal of battery; - = negative terminal of battery

1) Forward Biased
2) Reverse Biased

2.4.1 Forward Biased

The term *bias* used in electronics refers to a dc voltage that is maintained in a device by some externally connected source. When the p-side is connected to the positive terminal of the battery and n-side is connected to the negative terminal of the battery, the $p-n$ junction is said to be forward biased. In this situation, the external potential difference tends to cancel the internal potential barrier. The barrier is reduced in height, so diffusion current is enhanced. Therefore, current flows with relative ease through the junction. The driving force is such as to pull the electrons towards the positive anode and holes to the negative cathode. Both of these constitute current flow, but notice, holes are being pulled from where there are lots of holes, and electrons from where there are lots of electrons, and so we obtain a large current. A current of the order of a few milliamperes begins to flow across the $p-n$ junction when the external potential difference overcomes the potential barrier. For germanium potential barrier is about 0.3 volts and for silicon 0.7 volts.

2.4.2 Reverse Biased

When p-side is connected to the negative terminal of the battery and n-side is connected t the positive terminal of the battery, the $p-n$ junction is said to be reverse biased. In this situation, the holes are pulled from where there are very few and electrons from where there are very few. There is almost no current in the reverse biased $p-n$ junction.
Similar situation can be observed in firing of neuron. When an input pulse greater than threshold potential is applied on the dendrite of a neuron, it generates an electrical pulse in the form of action potential. Therefore, the barrier potential of $p-n$ junction can be compared with the threshold potential of neuron.
The $p-n$ junction is non-linear device because its resistance varies with external potential difference, therefore Ohm's law is not applicable on $p-n$ junction. The current voltage characteristic equation for $p-n$ junction can be expressed as;

$$I = I_s(e^{\frac{eV}{kT}} - 1) \tag{2.7}$$

Where I is current through $p-n$ junction, I_s is reverse saturation current, e is the base of natural logarithms ($e = 2.71828...$), e in the power is charge on electron ($e = 1.602 \times 10^{-19} C$), V is external applied potential difference, k is Boltzmann's constant and T is absolute temperature.
The $p-n$ junction is non-linear device as indicated by equation (2.7), however, by applying power series expansion we can convert the exponential function into linear function. In that case we can apply the linear approximation in a certain range of values where $p-n$ junction shows constant resistance and Ohm's law is valid for that region of operation.

2.5 Actifier

The combination of amplifier and rectifier ($p-n$ junction) is called actifier. Amplifier increases the input voltage level and rectifier generates unidirectional current in the circuit

depending upon the polarity of amplified voltage. Consider neuron membrane at equilibrium state, such that positive charge is distributed outside the membrane and negative charge is inside the membrane. Upon receiving a small input stimulation of about +30 millivolts, there is a change of 100 millivolts in the membrane potential. Moreover, the pulse always propagates in one direction from cell body to the axon of neuron. Due to the generation of amplified and unidirectional pulse, a neuron can be modeled by an actifier (figure 2.7).

Consider a voltage source is connected to the non-inverting input of the operational am-

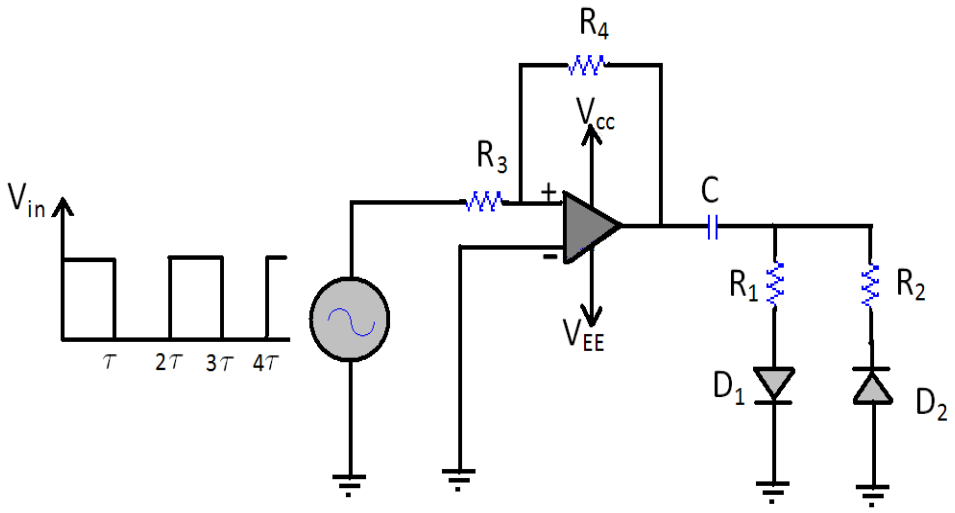

Figure 2.7: Electrical Model of Neuron

plifier. The operational amplifier in non-inverting configuration generates the amplified copy of the input. This amplified output of the operational amplifier is applied as input to the capacitor C in series with $p-n$ junction diode as shown in figure 2.7. The voltage source has a rectangular waveform with time period of 2τ. When a pulse of about 20 millivolts is applied as input on non-inverting input of the operational amplifier, it amplifies the pulse to its particular level defined by the values of R_3 and R_4. The capacitor gets fully charged due to this amplified pulse through resistance R_2. When voltage across D_1 exceeds from its threshold level, it becomes forward biased and capacitor discharges through resistance R_1. The combination of resistance and capacitance creates time constant for charging and discharging phases of the circuit.

By applying KVL around the capacitor and diode branch,

$$V_c + V_R = 0$$

$$V_c = -iR_1$$

$$i = i_c = c\frac{dv}{dt}$$

$$V = -R_1 C \frac{dv}{dt}$$

The solution of above equation can be written as

$$V(t) = V_o e^{-\frac{t}{R_1 C}}$$

Let

$$T_1 = R_1 C$$

So

$$V(t) = V_o e^{-\frac{t}{T_1}}$$

As a consequence, at the end of each half cycle, the capacitor is practically completely charged or completely discharged. The waveform of voltage across capacitor is given in figure 2.8.

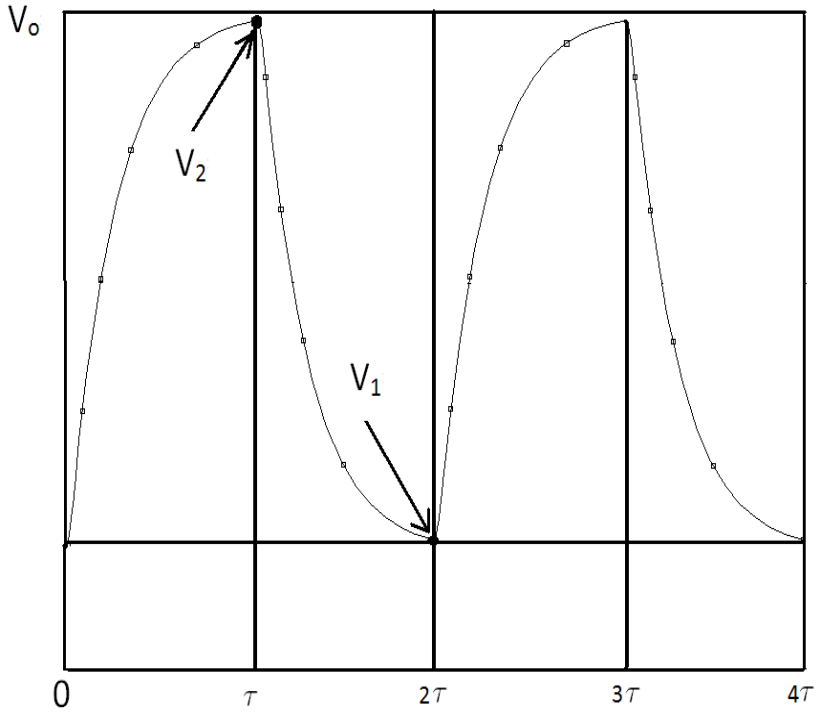

Figure 2.8: Charging and Discharging of Capacitor

Similarly, it can be shown that the output voltage is given by equation (2.8).

$$V(t) = \begin{cases} V_o e^{-\frac{t}{T_1}} & ;\ 0 \leq t \leq \tau \\ -V_o e^{-\frac{t-\tau}{T_2}} & ;\ \tau \leq t \leq 2\tau \end{cases} \tag{2.8}$$

In general equation (2.8) can be written as equation (2.9).

$$V(t) = \sum_{n=0}^{\infty} (-1)^n V_o e^{-\frac{t-n\tau}{T_{(n \mod 2)+1}}} \tag{2.9}$$

Assume that T_1 and T_2 are of a magnitude comparable to τ, so that in alternate half cycles, the capacitor is neither completely charged nor discharged. However, as time proceeds, the voltage across the capacitor will reach a steady state.

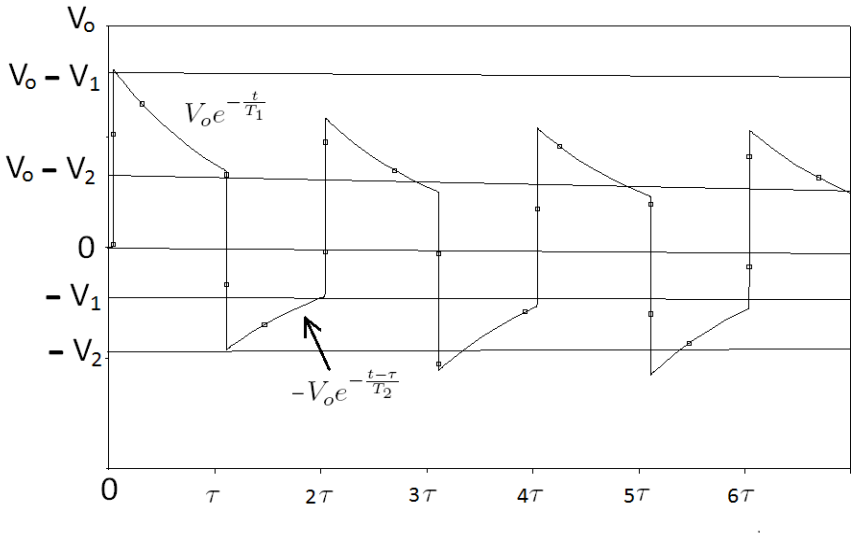

Figure 2.9: output waveform

Chapter 3

Neuron Actifier Model

Neurons are the excitable cells that can amplify a small input voltage signal. Based on this fact, we can model the electrical behavior of neuron by an amplifier. Moreover, a neuron also generates unidirectional current, therefore, we can approximate the generation of action potential of neuron by actifier. In this chapter we shall relate the behavior of actifier model with actual dynamics of excitable cells.

3.1 Neuron

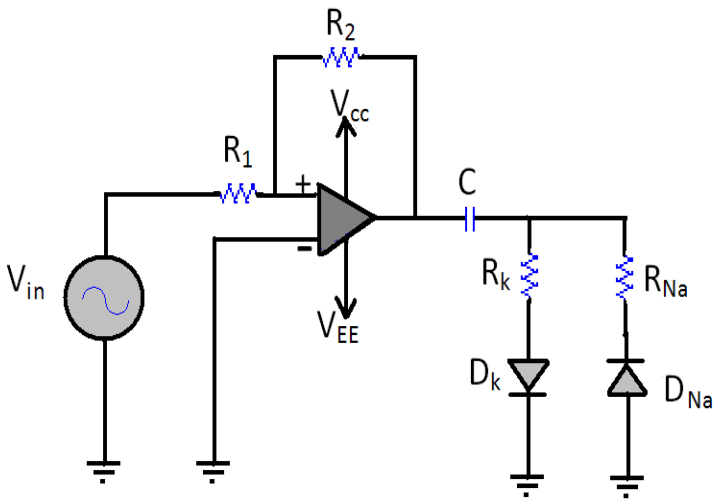

Figure 3.1: Neuron Circuit

Consider the circuit shown in figure 3.1 in which we modeled a neuron by variable capacitance, resistance and diodes. Neuron contains negatively charged protein molecules which are fixed inside the cell. Hence, protein acts as substrate in the formation of $p-n$ junction type structure between protein and the K^{+1} ions. The junction formed between protein molecules and the K^{+1} ions is called K-Junction. The potential barrier for K-Junction is about $V_k = 35mV$. Outside the cell, Na^{+1} ions are in higher concentration. These ions forms the N-Junction with protein molecules. The potential barrier for N-Junction is about $V_{Na} = -30mV$. These junctions are similar to ion channels as in Hodgkin-Huxley Model [20].
When an input pulse of about 20 or 30 millivolt appears on the input of operational amplifier, it generates an amplified pulse as an input for capacitor. The capacitor charges to its peak value depending upon the strength of input applied on it. As long as the voltage across diode D_k becomes greater than the potential barrier $V_k = 35mV$, the diode becomes forward biased and allows the capacitor to discharge. This phenomenon is equivalent to the movement of K^{+1} ions outside the cell. The conductance for outside movement of K^{+1} ions is g_k. At the same time when D_k is forward biased, D_{Na} is reverse biased. Since the junction in reverse biased condition is active for minority charge carriers, hence when D_k is active for the movement of K^{+1} ions outside the cell at the same time D_{Na} is active for the movement of leaky ions inside the cell.
When the voltage across D_k goes negative, it becomes reverse biased and K-Junction is closed for further movement of K^{+1} ions. When the voltage reaches at $V_{Na} = -30mV$, the diode D_{Na} becomes forward biased and Na^{+1} ions moves inside the cell. The conductance for inside movement of Na^{+1} ions is g_{Na}. At the same time when D_{Na} is forward biased, D_K is reverse biased. Hence, when D_{Na} is active for the movement of Na^{+1} ions inside the cell at the same time D_K is active for the movement of leaky ions outside the cell. The time constants for K^{+1} ions and Na^{+1} ions can be written as;

$$T_k = R_k C$$

$$T_{Na} = R_{Na} C$$

We can adjust the values of R and C according to the waveform of interest for a certain cell. For neuron, equation (2.9) can be written as equation (3.1).

$$V(t) = \begin{cases} V_o e^{-\frac{t-2n\tau}{T_k}} & ;\ 2n\tau \leq t \leq (2n+1)\tau \\ -V_o e^{-\frac{t-(2n+1)\tau}{T_{Na}}} & ;\ (2n+1)\tau \leq t \leq 2(n+1)\tau \end{cases} \tag{3.1}$$

In general equation (3.1) can be written as equation (3.2).

$$V(t) = V_o \sum_{n=0}^{\infty} [e^{-\frac{t-2n\tau}{T_k}} - e^{-\frac{t-(2n+1)\tau}{T_{Na}}}] \tag{3.2}$$

Equation (3.2) is referred as Neuron Action Potential (NAP) Equation. The circuit with actual 80 millivolts action potential is shown in figure 3.3 and the output of circuit is shown in figure 3.4.

This section illustrates the behavior of individual spiking neuron in response to simple pulses of dc voltage [25]. In all the diagrams that show the behavior of bursting, we have used an extra timer circuit (Figure 3.5).

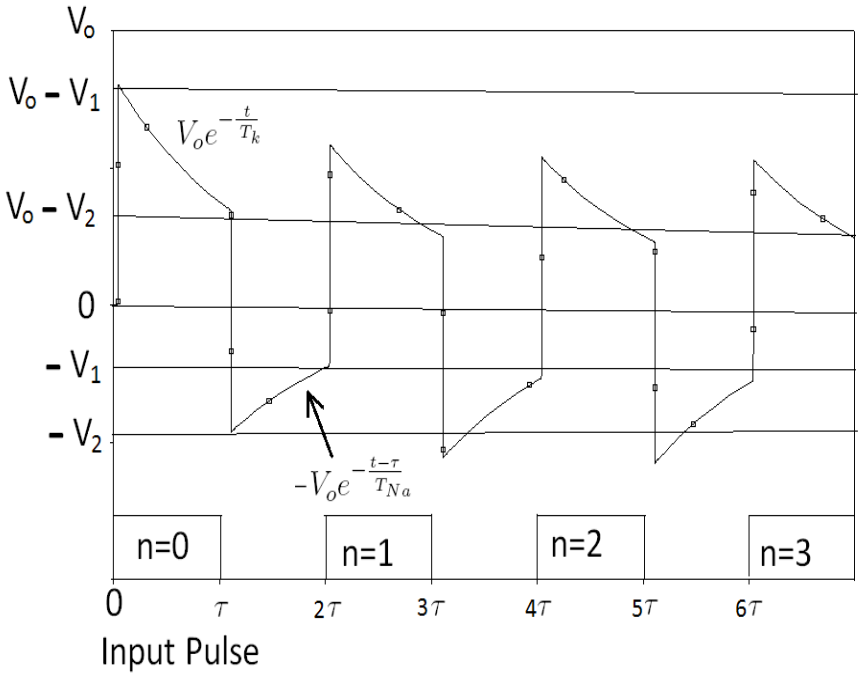

Figure 3.2: Input and output for neuron circuit

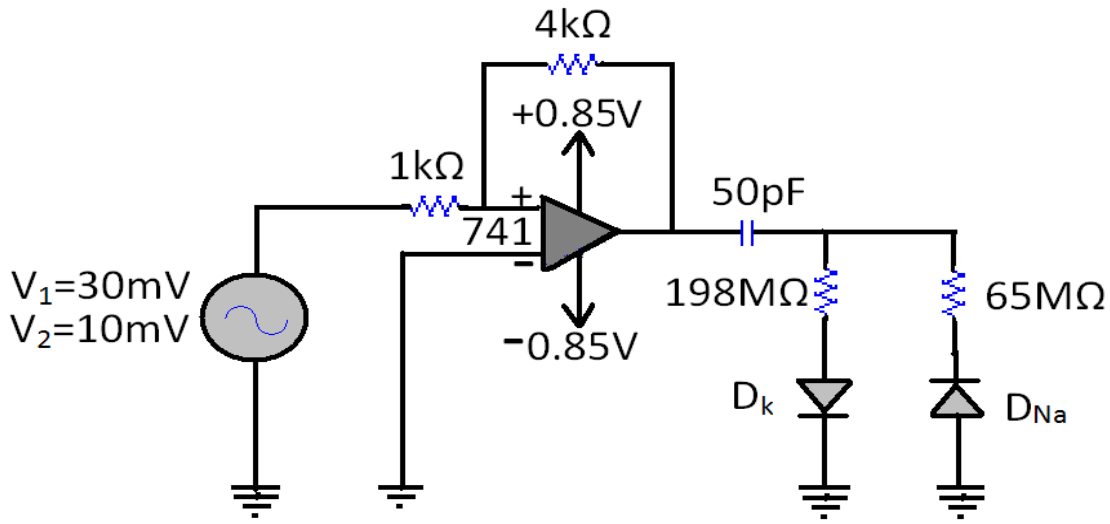

Figure 3.3: 80 millivolts action potential neuron circuit

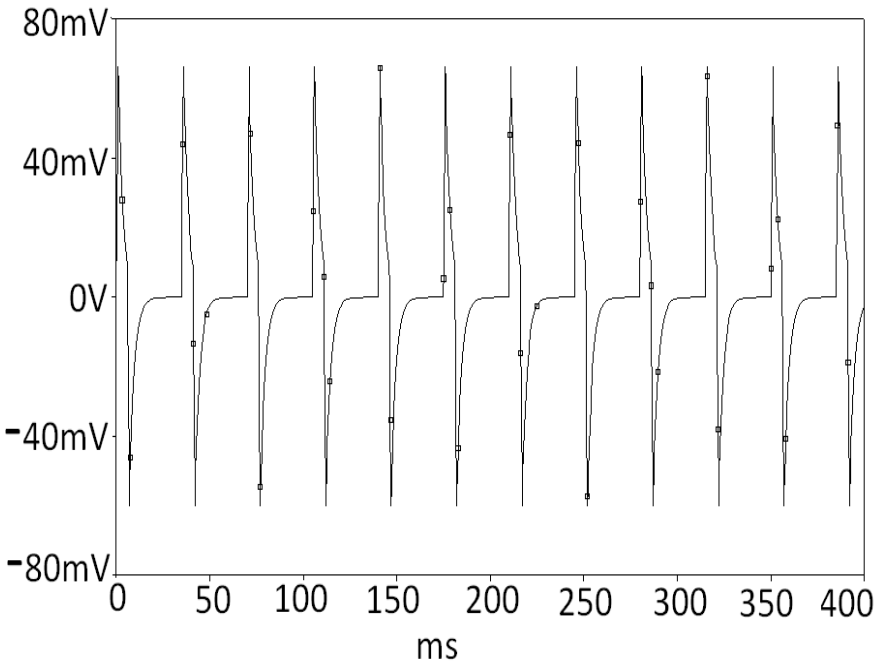

Figure 3.4: 80 millivolts action potential pulses

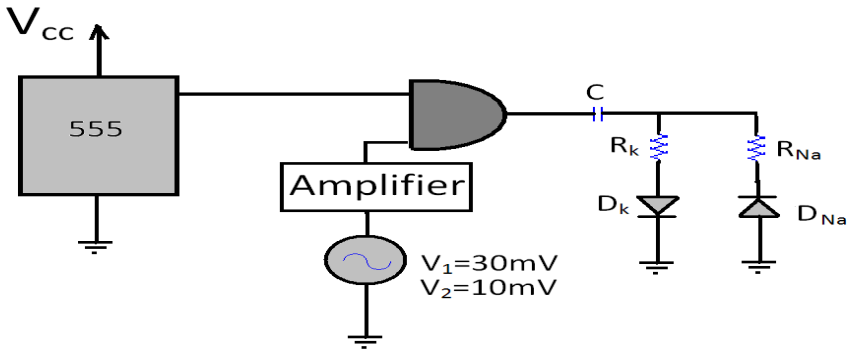

Figure 3.5: For Bursting and Regular Spiking we used Timer Circuit as an extra unit with source as : $V_1 = 30mV$, $V_2 = 10mV$, $V_{cc} = 8V$

3.2 Results

In this section we shall relate the experimental data to the simulation results. We can record the action potential of single neuron in awake mice using tetrodes. The tetrodes are injected in the mice brain through surgery and data is stored in computer memory to get the electrical behavior of mice brain neurons (figure 3.6).
The results of figure 3.6 can be described theoretically by AJ model.

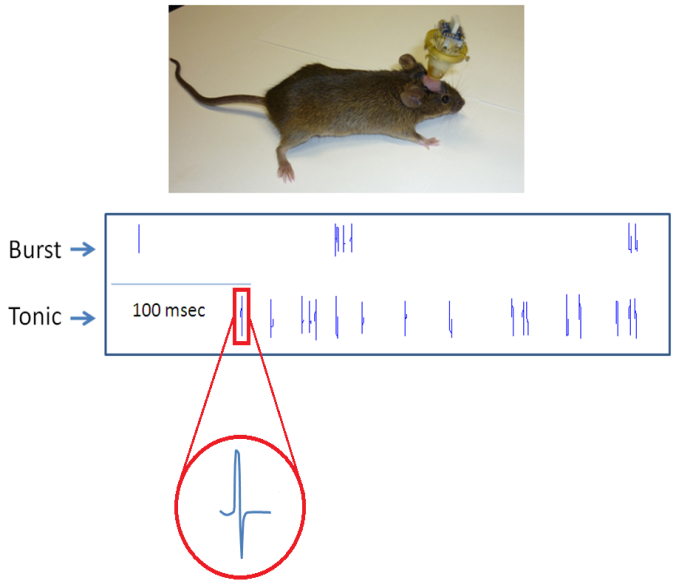

Figure 3.6: Action potential recording of single neuron in awake mice using tetrode

Tonic Spiking (TS): This type of behavior can be tested by applying constant dc input stimulus to the neuron. Initially the firing rate of neuron is very fast however as the time proceeds, its firing patterns are regularly spaced. Such behavior is called tonic spiking [24]. For tonic spiking, we used timer in free running state called astable mode. We also used function generator an AND gate. This complete arrangement gives us suitable stimulation for tonic spiking (figure 3.7).

Phasic Spiking (PS): In phasic spiking a neuron can fire a single spike at the beginning of the stimulation and remains stationary for the remaining interval of time [12, 22]. This behavior is shown in figure 3.8.

Tonic Bursting (TB): Some neurons, such as chattering neurons in cat neocortex, fire periodic bursts of spikes when stimulated (figure 3.9). The burst frequency may be 50 Hz. Such neurons contribute to the gamma-frequency oscillations in the brain [13, 21].

Phasic Bursting (PB): When stimulus is applied some neurons in the brain fires a

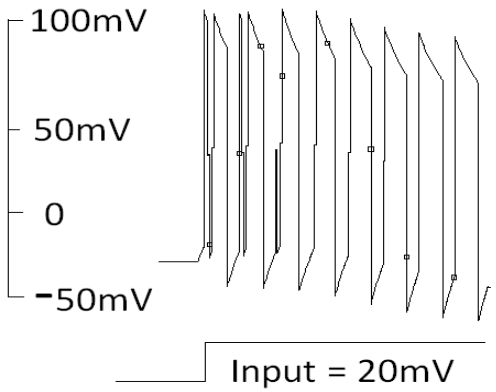

Figure 3.7: Tonic Spiking

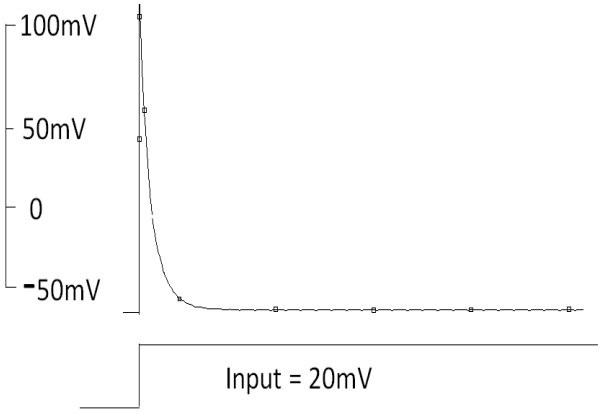

Figure 3.8: Phasic Spiking

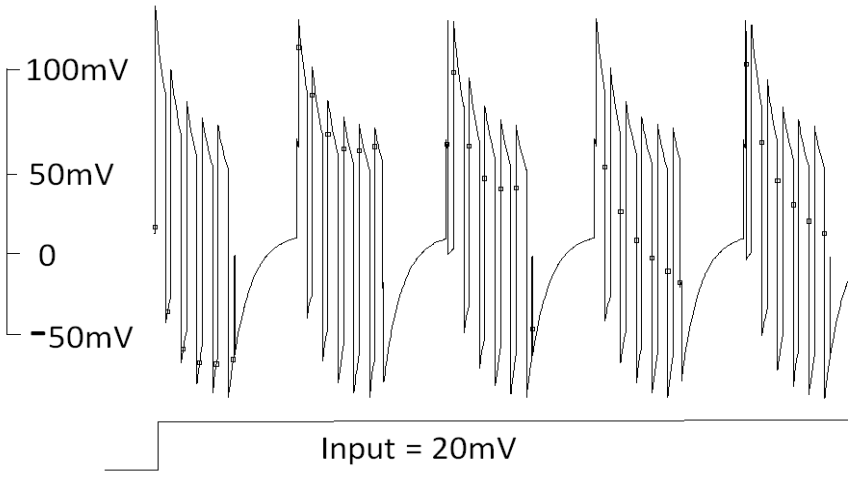

Figure 3.9: Tonic Bursting

train of continuous spikes. This behavior is called phasic bursting (figure 3.10). This is a very important behavior and cannot be neglected in the neuron model [48, 34].

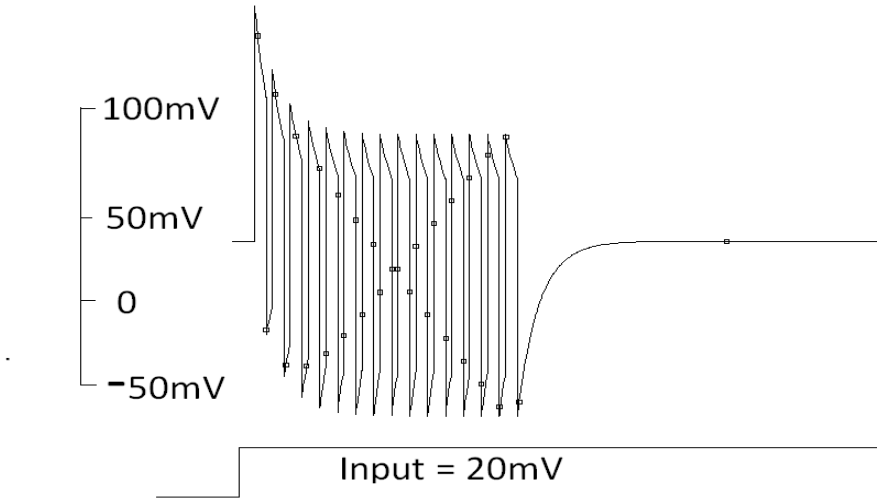

Figure 3.10: Phasic Bursting

Mixed Mode (MM): This type of neurons fires a burst at the beginning of the stimulation and behaves like tonic spiking mode (figure 3.11). This type of neurons are found in mammalian neocortex [52].

Spike Frequency Adaptation (SFA): This type of neurons are commonly found in mammalian neocortex (figure 3.12). Initially they fires at high frequency and can

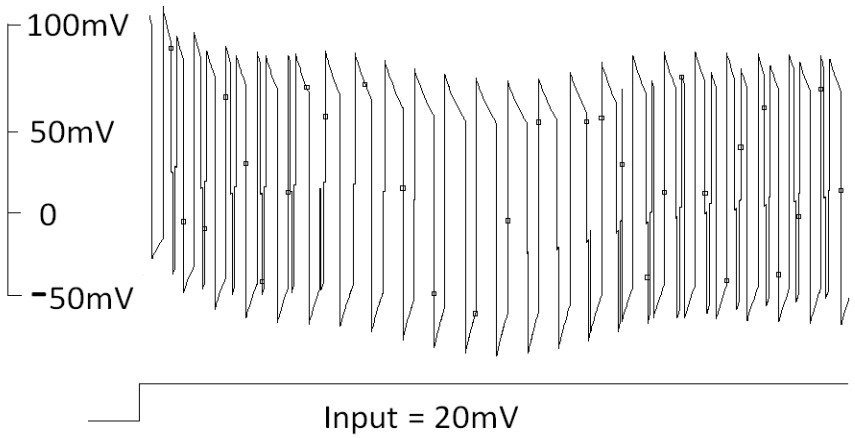

Figure 3.11: Mixed Mode (Bursting Then Spiking)

sustain a stable frequency of firing [23].

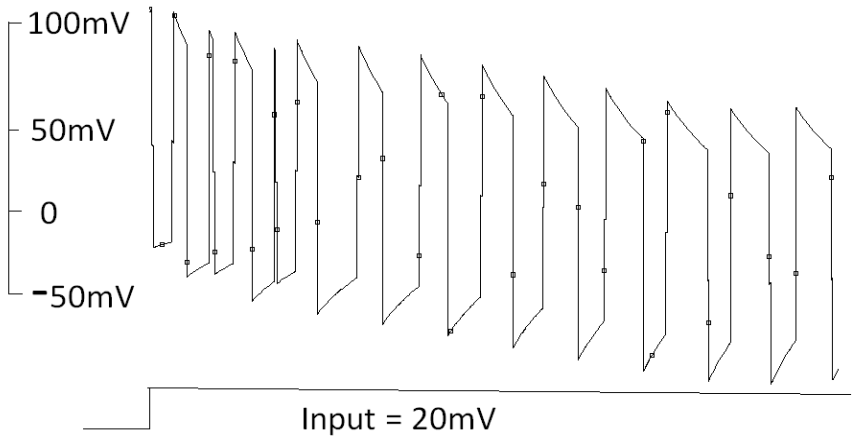

Figure 3.12: Spike Frequency Adaptation

Class 1 Excitability (C-1): The frequency of firing of this type of neurons depends on the strength of the input (figure 3.13). They fire low frequency spikes when input is weak and fire at high frequency when stimulation strength is greater. We can predict the strength of input by firing rate of the class-1 excitable neurons [31].

Class 2 Excitability (C-2): This type of neurons fires equally spaced spikes as the signal strength is increased (figure 3.14). So the firing frequency of such neurons is independent of the signal strength [39, 29, 2].

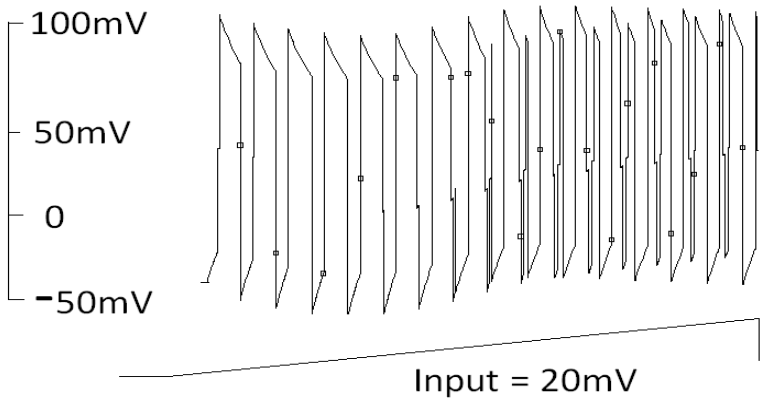

Figure 3.13: Class 1 Excitability

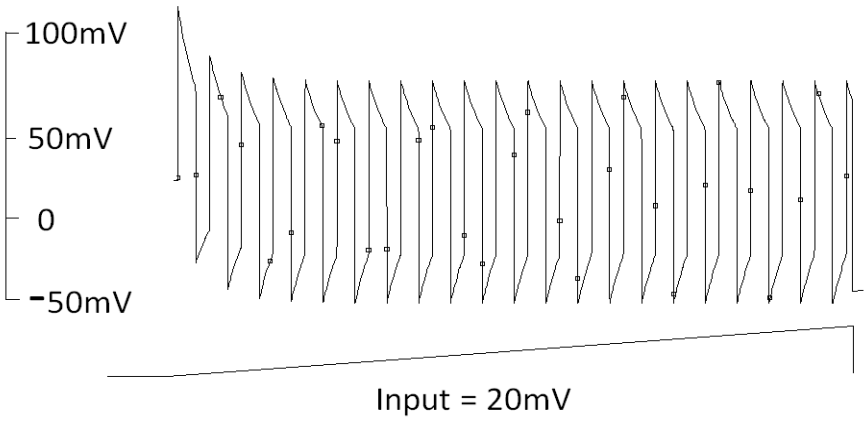

Figure 3.14: Class 2 Excitability

Spike Latency (SL): This type of cortical neurons fire spikes with a delay that depends on the strength of the input signal and are called spike latency firing neurons (figure 3.15).

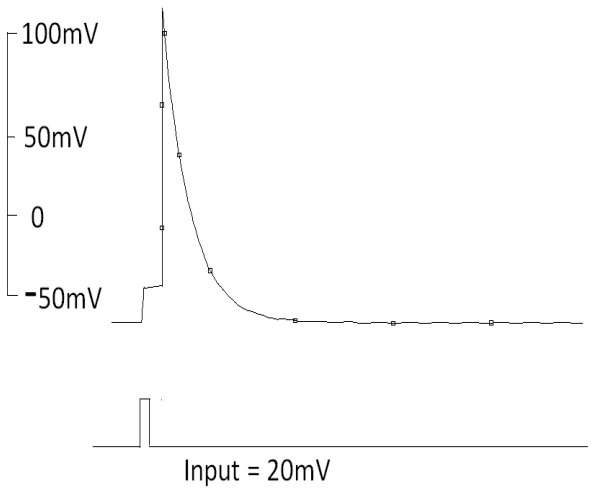

Figure 3.15: Spike Latency

Subthreshold Oscillations (SO): Practically every brain structure has oscillatory neuron potentials (figure 3.16) . The frequency of such oscillations enforces neurons to act as bandpass filters [18, 19].

Frequency Preference and Resonance (R): Some neurons shows the phenomenon of resonance. The neuron can fire only if the frequency of stimulation lies within a certain range (figure 3.17). If the gap between two stimulation pulses is very short or very large, the neuron will not fire until it matches certain frequency called resonance frequency determined by RC-time constant of the circuit. Such neurons are called resonators [35, 36].

Integration and Coincidence Detection (I): This type of neurons fire at high frequencies when the time interval between two input pulses is less than RC-time constant of the circuit (figure 3.18). These neurons are helpful in detecting high frequency stimulus [54, 55, 5].

Rebound Spike (RS): These are inhibitory type of neurons (figure 3.19). When these neurons captures an inhibitory input pulse, they fires a post inhibitory spike [47].

Rebound Burst (RB): This type of neurons includes the thalamo-cortical cells and may fire post-inhibitory bursts (figure 3.20). Such type of bursts contribute to the sleep oscillations in thalamo-cortical system [47].

Threshold Variability (TV): The biological neurons have a variable threshold that depends on previous activity of the neurons (figure 3.21). We can first stimulate a neuron with a small excitatory pulse so that the neuron does not fire. After a

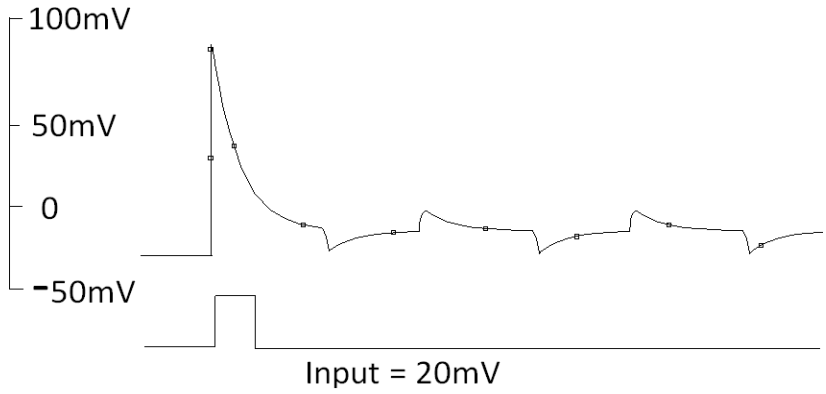

Figure 3.16: Subthreshold Oscillations

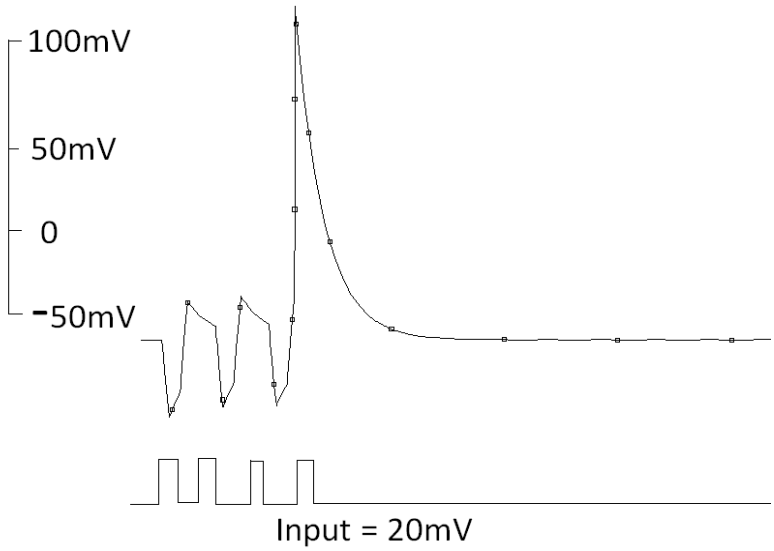

Figure 3.17: Resonator: $V_1 = -30mV$, $V_2 = 10mV$, $V_{cc} = 1V$, $V_{EE} = -1V$

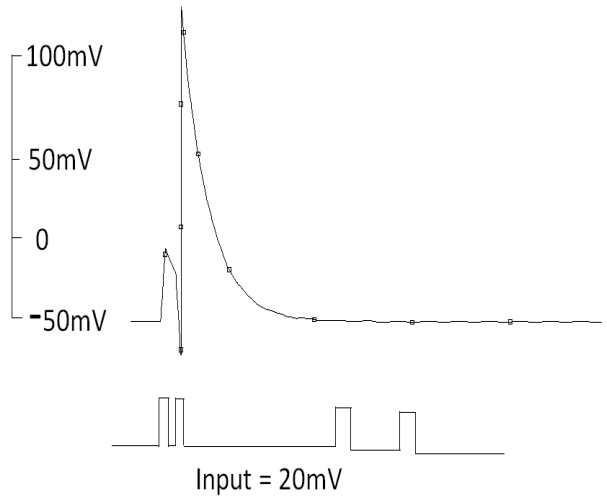

Figure 3.18: Integrator

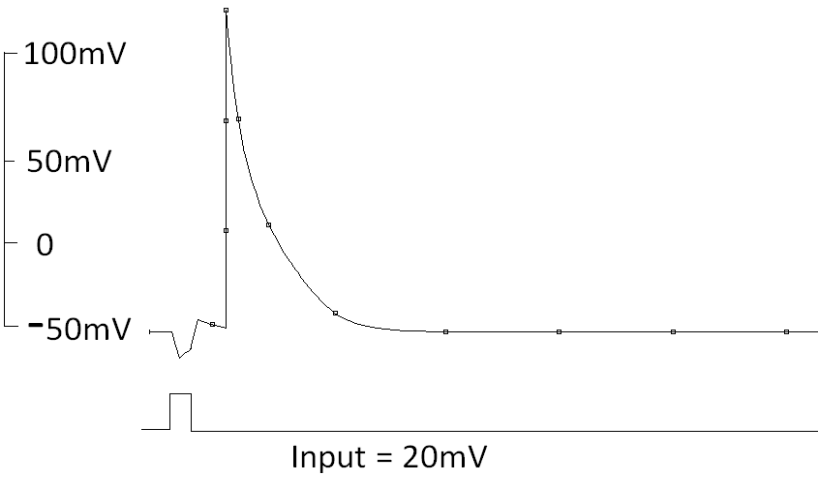

Figure 3.19: Rebound Spiking: $V_1 = -30mV$, $V_2 = 10mV$, $V_{cc} = 5V$, $V_{EE} = -1V$

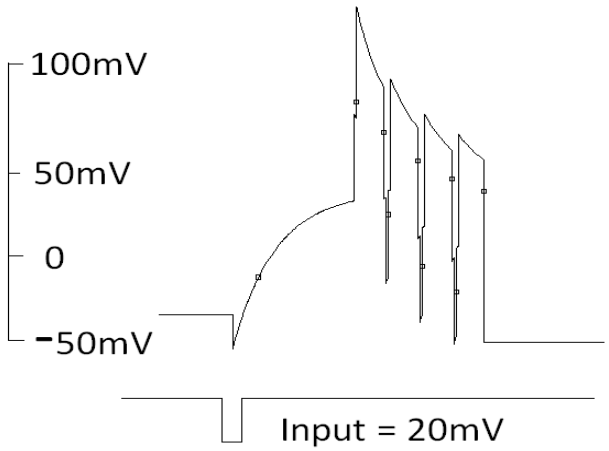

Figure 3.20: Rebound Burst

while, we apply a brief inhibitory input and exactly the same subthreshold pulse. The neuron fires the second time because its threshold was lowered by the preceding inhibitory input. This phenomenon is called threshold variability [3].

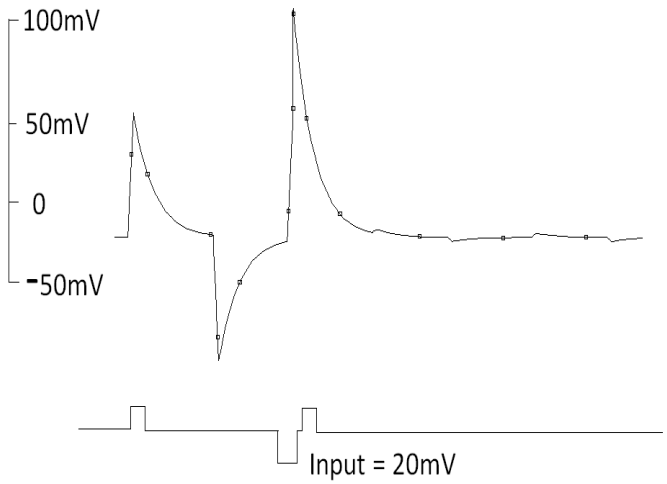

Figure 3.21: Threshold Variability

Bistability of Resting and Spiking States (B): Some neurons show two stable modes of operation: resting and tonic spiking (figure 3.22). An excitatory or inhibitory pulse can switch between these modes. Initially when stimulation is applied, the neuron shows tonic spiking or even bursting and by applying same input second time that exhibits resting [44, 4].

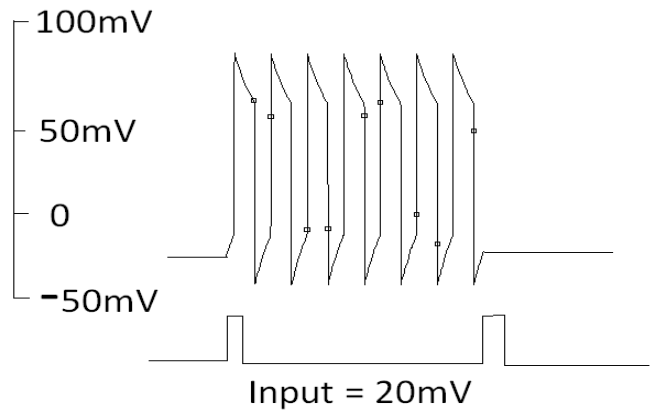

Figure 3.22: Bistability of Resting and Spiking States

Depolarization After Potential (DAP): After firing a spike, the membrane potential of a neuron may show a depolarization state (figure 3.23).This type of behavior is called depolarization after-potential (DAP) [51].

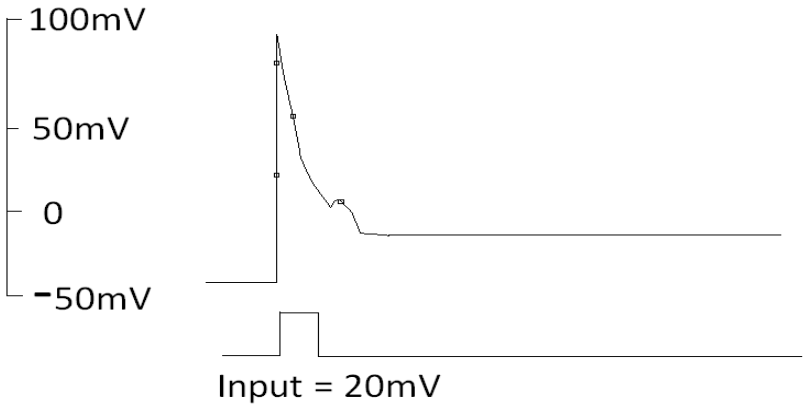

Figure 3.23: Depolarization After Potential

Accommodation (A): Neurons are extremely sensitive to high frequency inputs, but may not fire in response to a strong but slowly increasing input (figure 3.24). When a slowly increasing ramped input is applied, the neuron initially fires bumps but as the coincident pulse appears as input, it fires [43].

Inhibition-Induced Spiking (IIS): This type of behavior can be observed in many

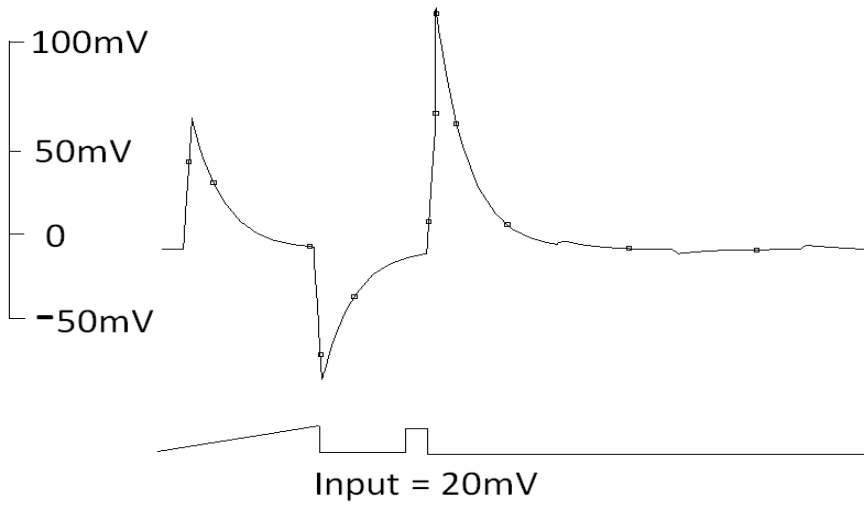

Figure 3.24: Neuron Accommodation

thalamo-cortical neurons (figure 3.25). This type of neurons remains stationary in the presence of input and fires spikes when input is absent [42].

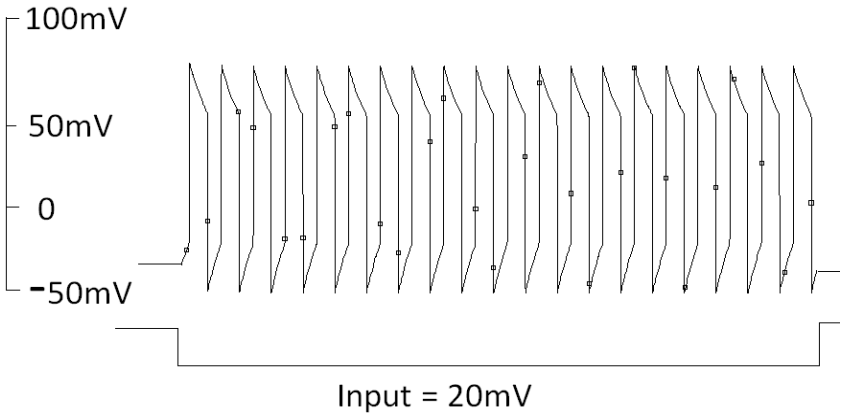

Figure 3.25: Inhibition-Induced Spiking

Inhibition-Induced Bursting (IIB): Instead of spiking, a thalamo-cortical neuron can fire bursts of spikes when input is absent (figure 3.26). This type of behavior is called inhibition induced bursting. This behavior plays an important role in sleep rhythms [41].

Chaos in Neuron (CN): Some neurons fires random pulses when excited by identical pulses (figure 3.27). This type of behavior is called neuron chaos [40, 38, 45, 37].

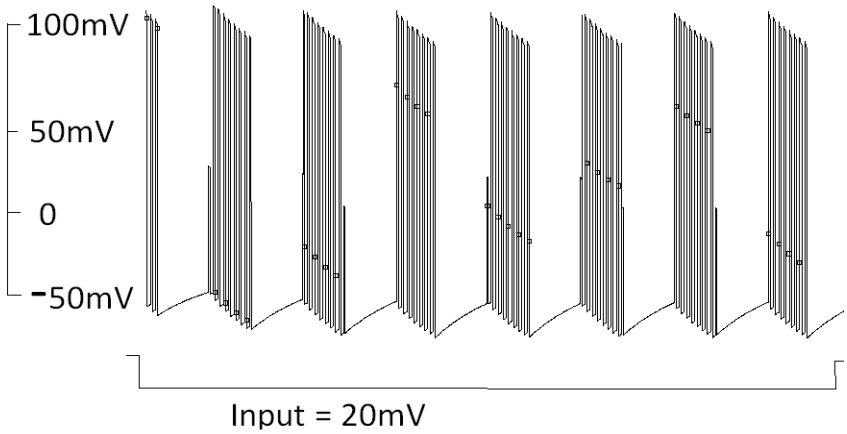

Figure 3.26: Inhibition-Induced Bursting

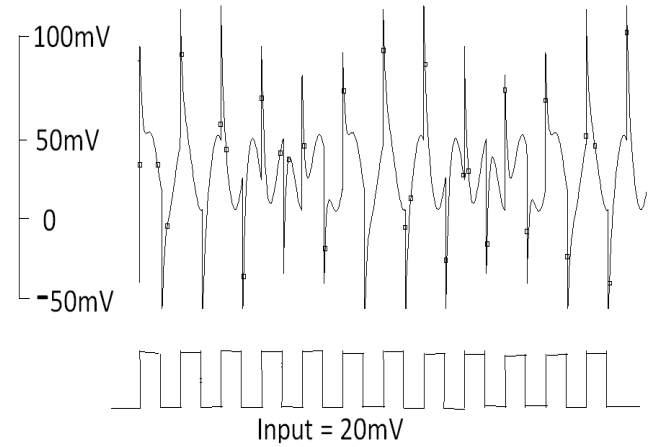

Figure 3.27: Chaos in Neuron

Spike Bursting (SB): This type of behavior is observed in the mouse brain neurons [37]. The neuron fires spikes and burst simultaneously (3.28).

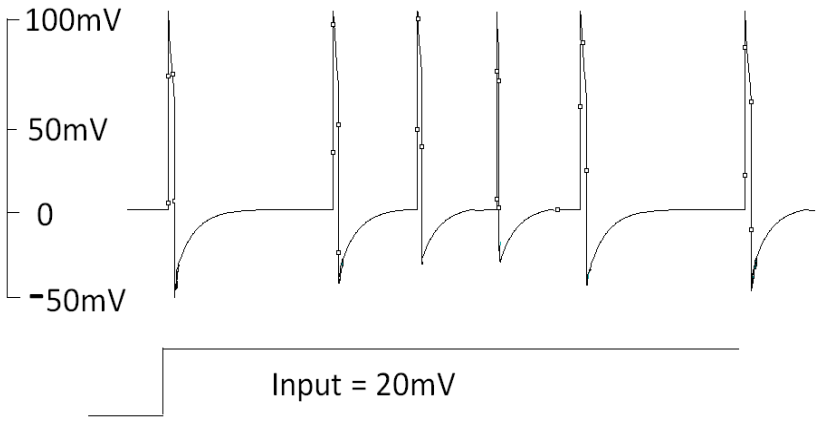

Figure 3.28: Spike Bursting

No model should exhibit all these 22 behaviors at the same time because some of the properties are mutually exclusive. For example, a neuron cannot be an integrator and resonator at the same time. However, there are models that can easily be tuned to exhibit each such property. The figures presented here are obtained by using PSPICE 9.2 LITE EDITION. In case of bursting we used an additional circuit of timer and function generator to get the desired output waveform.

3.3 comparison

In table II, we presented comparison of different models. For neurons, AJ-Model takes 12 FLOPS while for cardiac myocyte it takes 15 FLOPS.

Table 3.1: **Comparison with other models.**

Models	BM	TS	PS	TB	PB	MM	SFA	C-1	C-2	SL	SO	R	I	RS	RB	TV	B	DAP	A	IIS	IIB	C	SB	M	FLOPs
Integrate and Fire	-	+	-	-	-	-	-	+	-	-	-	-	+	-	-	-	-	-	-	-	-	-		-	5
Integrate and Fire with adapt.	-	+	-	-	-	-	+	+	-	-	-	-	+	-	-	-	-	+	-	-	-	-		-	10
Integrate and Fire-or-burst	-	+	+	-	+	-	+	+	-	-	-	-	+	+	+	-	+	+	-	-	-	-		-	13
Resonate and Fire	-	+	+	-	-	-	-	+	+	-	+	+	+	+	-	-	+	+	+	-	-	+		-	10
Quadratic Integrate and Fire	-	+	-	-	-	-	-	+	-	+	-	-	+	-	-	+	+	-	-	-	-	-		-	7
Izhikevich (2003)	-	+	+	+	+	+	+	+	+	+	+	+	+	+	+	+	+	+	+	+	+	+		-	13
FitzHugh-Nagumo	-	+	+	-		-	-	+	-	+	+	+	-	-	-	+	+	-	+	+	-	-		-	72
Hindmarsh-Rose	-	+	+	+			+	+	+	+	+	+	+	+	+	+	+	+	+	+		+		-	120
Morris-lecar	+	+	+	-		-	-	+	+	+	+	+	+	-	-	+	+	-	+	+	-	-		-	600
Wilson	-	+	+	+			+	+	+	+	+	+	+	-	+	+	-	+	+					-	180
Hodgkin-Huxley	+	+	+	+			+	+	+	+	+	+	+	+	+	+	+	+	+	+		+		-	1200
Asif-Jamil Model (2013)	+	+	+	+	+	+	+	+	+	+	+	+	+	+	+	+	+	+	+	+	+	+	+	+	**12**

This table compares all the well known models of neurons with AJ-model. BM stands for Biophysically Meaningful, M stands for myocyte and other column headings are stated in the result section. The empty cells in the table represent that information about corresponding behaviors are not available.

Part II

Cardiac Myocyte

Chapter 4

Cardiac Myocyte Modeling

4.1 Luo-Rudy Model

Luo and Rudy presented in 1991, the first cardiac action potential model for Guinea pig. This model was based upon the previously proposed Hodgkin and Huxley model. The Luo-Rudy model can be expressed as;

$$\frac{dV}{dt} = -\frac{1}{C}(I_{Na} + I_K + I_{KI} + I_{KP} + I_B + I_{SI} + I_{st})$$

Where
C = membrane capacitance
I_{st} = stimulation current
I_{Na} = fast inward sodium current
I_K = time-dependent potassium current
I_{KI} = time-independent potassium current
I_{KP} = the plateau potassium current
I_B = the background current
I_{SI} = the slow inward calcium current
In Luo-Rudy model ionic currents are described by the Markov chain process. Markov chain process is a memoryless process in which all the information is confined in the present state, not on the previous history of the process. For any ionic channel x, we can attach three states as;
1) Opening state denoted by O
2) Closing state denoted by C
3) Inactivation state denoted by I
Let n be the total number of channels per unit area and O be the probability of opening of the channels, the current due to any arbitrary channel x can be expressed as;

$$I_x = \bar{g_x}.n.O.(V - E_x)$$

Where
$\bar{g_x}$ = Single channel conductance
$V - E_x$ = Effective force on ionic channel
The state transition of Luo-Rudy model are expressed in figure 4.1. Recently, some more

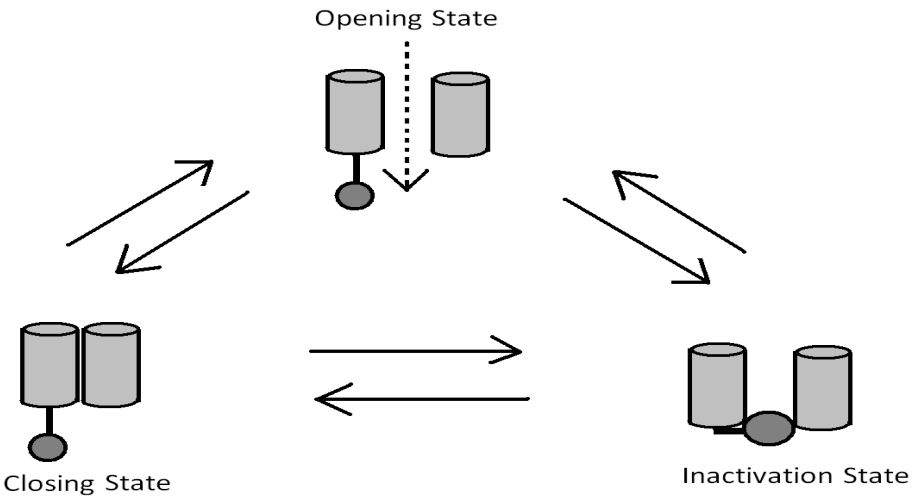

Figure 4.1: Markov chain based Luo-Rudy model representing the state transition between opening, closing and inactivation of ionic current channels

ionic channel currents are observed and Luo-Rudy model have been updated with currents like $I_{Ca(L)}$, I_{Ks}, I_{Kr} and I_{rel}. Due to the discovery of more ionic channel currents, the complexity of Luo-Rudy model tends to increase.

4.1.1 Cardiac Myocyte Modeling by Actifier

Consider the circuit shown in figure 4.2, which represents the cardiac myocyte. The difference between this circuit and the previous one shown in figure 3.1, is the ionic oscillator V_{ion}. This ionic oscillator represents the injection of Ca^{+2} ions in the heart cell. We modeled the Ca^{+2} ion concentration by normal distribution function.

Consider the voltage pulse is applied on capacitor C and it is charged to its peak value. As the voltage across D_K exceeds $V_k = 35mV$, it becomes forward biased and K^{+1} moves outside the cell. At the same time when K^{+1} is moving outside, V_{ion} provides voltage to D_{Na} to forward bias D_{Na}, and thus Ca^{+2} moves inside the cell.
Mathematically the action potential for cardiac myocyte can be written as equation (4.1),

$$V(t) = \begin{cases} V_1 e^{-\frac{t-2n\tau}{T_k}} + V_2 e^{-\frac{(t-(2n+1)\tau)^2}{T_{Na}}} ; 2n\tau \leq t \leq (2n+1)\tau \\ -V_o \qquad\qquad\qquad\qquad\quad ; (2n+1)\tau \leq t \leq 2(n+1)\tau \end{cases} \tag{4.1}$$

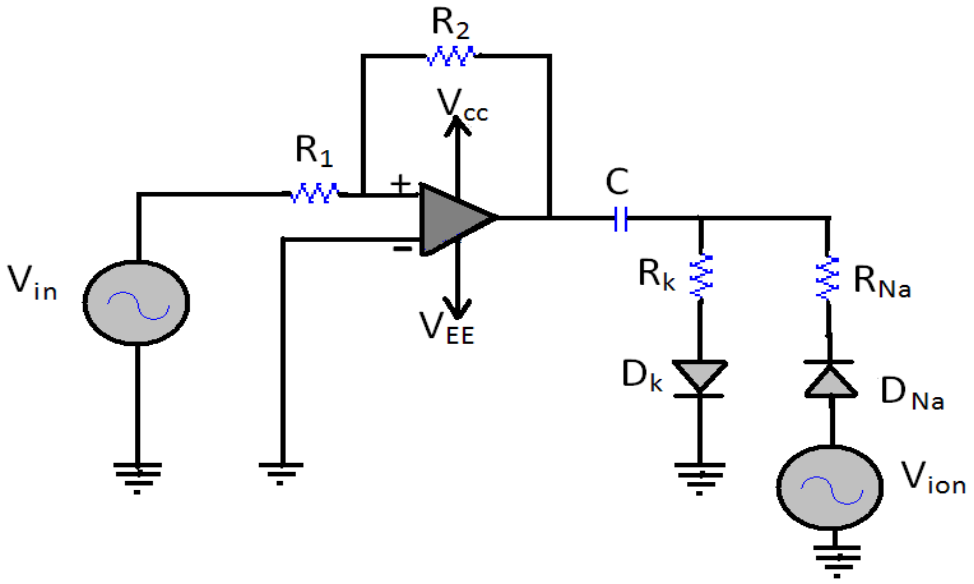

Figure 4.2: Cardiac Myocyte Circuit

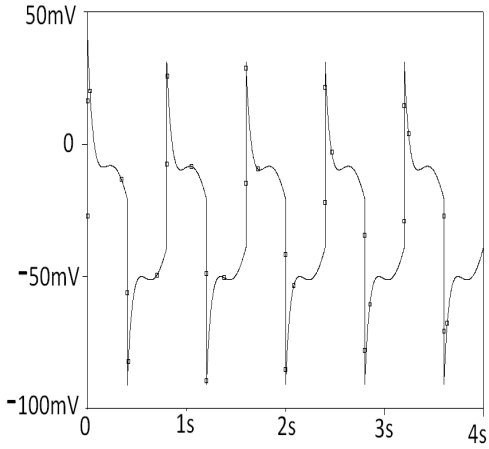

Figure 4.3: Cardiac myocyte action potential when inputs are adjusted as: V_{in} can be characterized by four parameters V_1, V_2, Pulse Width and Period. $V_1 = -1V$; $V_2 = 0.5V$; $Pulsewidth = 12cm0.4seconds$; $Period = 0.8seconds$; $R_1 = 1k\Omega$; $R_2 = 10k\Omega$; $V_{cc} = 0.42V$; $V_{EE} = -0.42V$; $C = 1.3pF$; $R_k = 198M\Omega$; $R_{Na} = 65M\Omega$; V_{ion} can be modeled by three parameters as $V_{offset} = -0.04V$; $V_{amplitude} = 0.03V$; $Frequency = 1.25Hz$

In general above equation can be written as equation (4.2);

$$V(t) = \sum_{n=0}^{\infty}[V_1 e^{-\frac{t-2n\tau}{T_k}} + V_2 e^{-\frac{(t-(2n+1)\tau)^2}{T_{Na}}} - V_o[u(t-(2n+1)\tau) - u(t-2(n+1)\tau)]] \tag{4.2}$$

V_1 and V_2 are the arbitrary constants. Equation (4.2) is referred as Cardiac Action Potential (CAP) Equation. In above equation (4.2), the term $V_2 e^{-\frac{(t-(2n+1)\tau)^2}{T_{Na}}}$ represents the Ca^{+2} ion concentration. Clearly, we can see that the Ca^{+2} ions concentration is represented by normal distribution function (figure 4.4).

The formation of cardiac action potential can be divided into three steps: 1) Inward

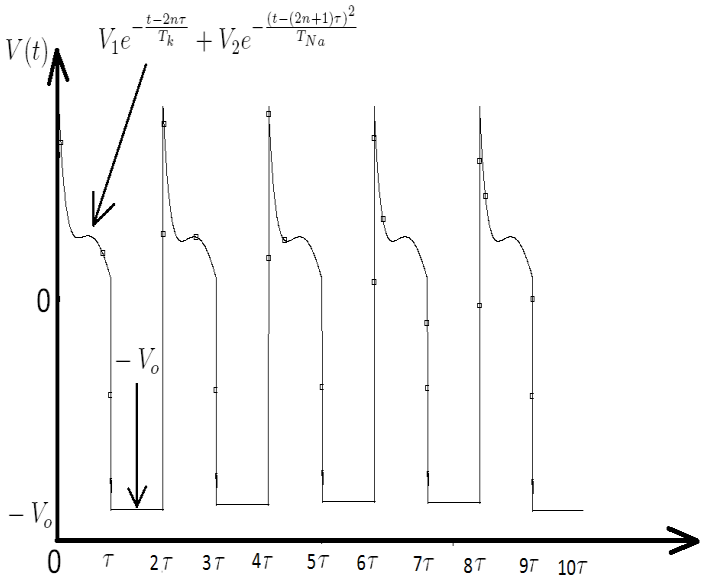

Figure 4.4: Cardiac Myocyte action potential

movement of sodium ions 2) Outward movement of potassium ions 3) Injection of calcium ions when potassium is moving outward. Typically cardiac myocyte action potential starts from -80 millivolts and goes to +35 millivolts. Due to inward movement of fast sodium ions, potential rapidly increases from -80 millivolts to +35 millivolts. When potential exceeds 35 millivolts, K-Junction goes in forward biased region and allows the potassium to move out of the cell. The slow movement of calcium into the cell causes plateau phase of the myocyte that distinguish it from neuron. This phase of the cardiac myocyte maintains the heart beat at constant level of 0.8 seconds [14]. Like other excitable cells, cardiac myocyte is also refractory for input stimulation. If a myocyte is in active region, in certain time interval it does not generate a new action potential. This time interval is

called refractory period. The refractory period of cardiac myocyte is about 50 milliseconds to 350 milliseconds. By slight variation we can show arrythmia in the cardiac myocytes that is caused by the excess of influx of the calcium ions (figure 4.5), which also confirms the actual experimental results [8].

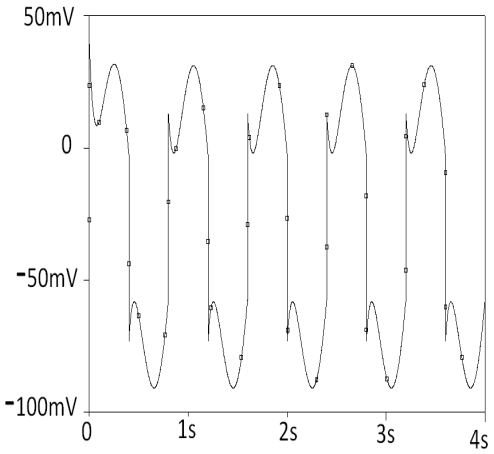

Figure 4.5: Cardiac myocyte action potential when inputs are adjusted as: V_{in} can be characterized by four parameters V_1, V_2, Pulse Width and Period. $V_1 = -1V$; $V_2 = 0.5V$; $Pulsewidth = 12cm0.4seconds$; $Period = 0.8seconds$; $R_1 = 1k\Omega$; $R_2 = 10k\Omega$; $V_{cc} = 0.42V$; $V_{EE} = -0.42V$; $C = 1.3pF$; $R_k = 198M\Omega$; $R_{Na} = 65M\Omega$; V_{ion} can be modeled by three parameters as $V_{offset} = -0.04V$; $V_{amplitude} = 0.09V$; $Frequency = 1.25Hz$

4.2 Results

The cardiac myocytes can fire action potential due to the mechanical impulses of excitation contraction process. Unlike neurons, the action potential of cardiac myocyte is prolong due to the presence of calcium ions as shown in figure 4.6. The action potential of cardiac myocyte can be divided into six phases as:
1) Stimulation
2) Upstroke
3) Early repolarization
4) Plateau
5) Final repolarization
6) Resting
The action potential of cardiac myocyte is generated by the electrical pulse coming from sinoatrial node, due to heart beat. When action potential is initiated, the re-excitation of cell cannot occur unless the first five phases of action potential are not completed, therefore, this interval is called absolute refractory period or Action Potential Duration (APD). During the end of final repolarization and resting, a new stimulation pulse can

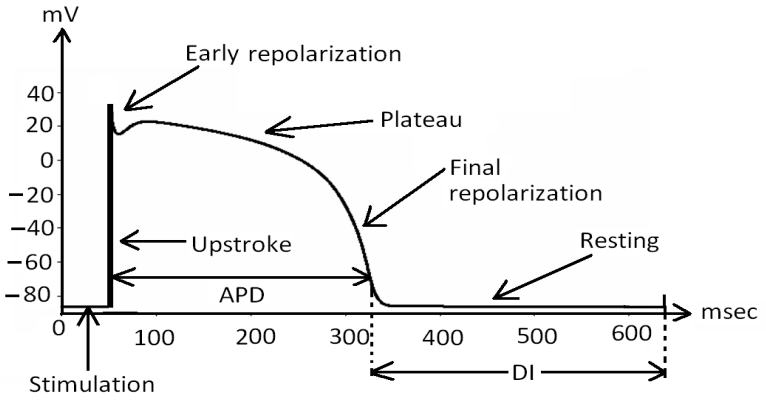

Figure 4.6: Cardiac myocyte action potential [1]

generate an action potential in the cell, therefore, this interval is called relative refractory period or Diastolic Interval (DI).

4.3 Restitution Function

The function which relates the Action Potential Duration (APD) and the Diastolic Interval (DI) is called APD Restitution Function. A graph drawn between APD and DI in such a way that DI is taken along x-axis and APD is taken along y-axis is called restitution curve. Restitution curve exhibits some properties that can be stated as:
1) It is an exponential curve.
2) The slope of restitution curve flattens when DI is 300 milliseconds, called critical point of restitution curve.
3) Restitution curve shifts towards negative slope after critical point.
4) At any instant, sum of x and y coordinate represents Basic Cycle Length (BCL).
5) BCL increases with increase in DI and after critical point it shifts toward the smaller values again.
6) The slope of restitution curve at any point gives the excitation rate.
We can represent the equations for APD and DI by considering the cardiac myocyte action potential curve as shown in figure 4.3 as,

$$APD = y(t) = \alpha e^{-\frac{t-\tau_1}{T_k}} + \beta e^{-\frac{(t-\tau_2)^2}{T_{Na}}} \tag{4.3}$$

$$DI = x(t) = \gamma e^{-\frac{(t-\tau_3)^2}{T_k}} \tag{4.4}$$

α represents the interval for outward flux (efflux) of potassium ions from the cell, β is the interval of inward flow (influx) of sodium ions into the cell and γ is reverse recovery interval of membrane for secondary excitation of cell. The value of γ is taken large enough due to the fact that, recovery process takes long time due to redistribution of ions across the membrane. From experimental data, we can choose the initial value α as 30 milliseconds to be consistent with experimental results [17]. The values of other parameter are;
$\alpha = 30msec$, $\beta = 150msec$, $\gamma = 350msec$, $\tau_1 = 0$, $\tau_2 = 20msec$, $\tau_3 = 15msec$, $T_k = 150msec$, $T_{Na} = 300msec$
The reason for above choice is straightforward from the fact that tubules of cardiac myocyte is 5 times greater than that of neurons. Moreover, note that the time constant for sodium ions is taken greater than potassium due to the presence of calcium.
Equations (4.3) and (4.4) represents the unbiased restitutio function. By considering the unbiased equations, we plotted the graph between APD and DI in such a way that APD is taken along y-axis and DI is taken along x-axis we get the following two graphs (figure 4.7 and figure 4.8).

MATLAB code for figure 4.7

```
t=[20:0.01:40];
x=350*exp(-(t-15).^2/150);
y=(30*(exp(-(t)/150)+150*exp(-(t-20).^2/300)))/(12*pi);
plot(x,y),xlabel('DI'),ylabel('APD'),grid
```

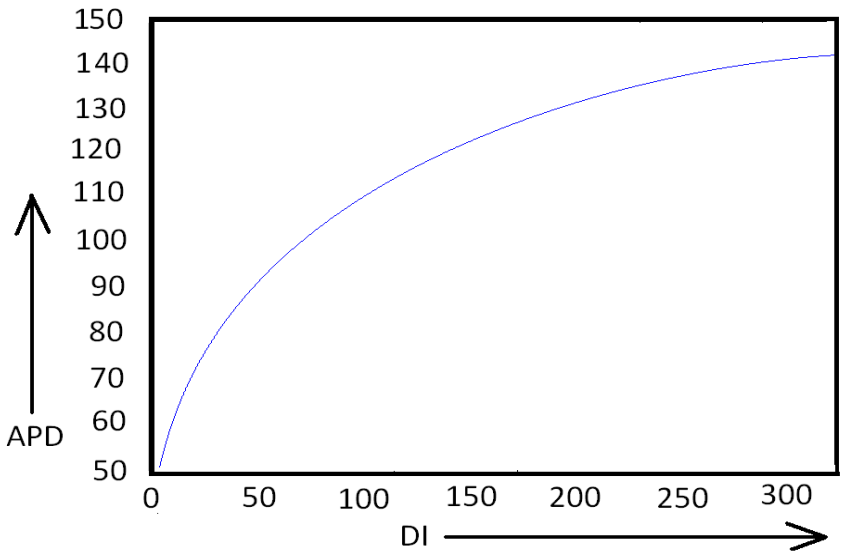

Figure 4.7: APD vs DI when $20msec \leq t \leq 40msec$

In figure 4.7 the relation between APD and DI is exponential which shows that, when value of DI increases initially, there is rapid increase in APD (i.e. the slope of graph is greater than 1) and finally restitution curve becomes almost parallel along x-axis [17]. The sum of APD and DI is called basic cycle length (BCL). When the value of DI is small, corresponding value of APD is also small, representing that if cell is excited in such a way that its DI is short, it will generate the next action potential with shorter APD, as

a result recovery time of cell also reduces and hence the BCL.

MATLAB code for figure 4.8

```
t=[0:0.01:40];
y=30*exp(-t/150)+150*exp(-(t-20).^2/300);
x=300*exp(-(t-15).^2/150);
plot(x,y),xlabel('DI'),ylabel('APD'),grid
```

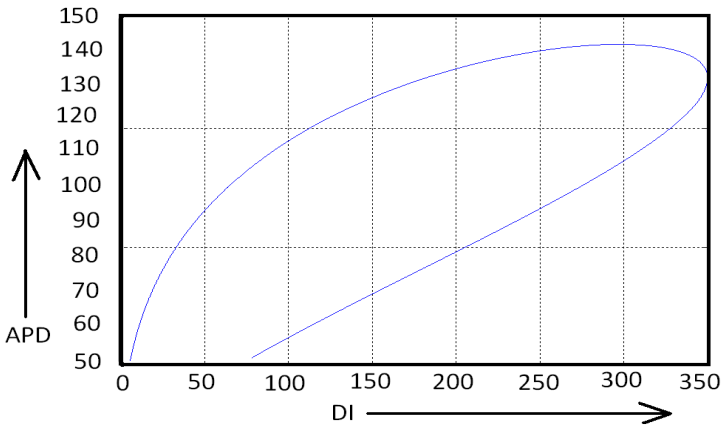

Figure 4.8: APD vs DI when $0 \leq t \leq 40msec$

The exponential increase in APD and DI occurs when $DI < 300$ *milliseconds* (figure 4.8). As the value of DI increases from 300 milliseconds, APD falls down to the lower values representing the negative slope. For detailed view of graph consider the 3D plot of APD and DI along time scale (figure 4.9).

MATLAB code for figure 4.9

```
t=[0:0.01:40];
x=350*exp(-(t-15).^2/150);
y=30*exp(-t/150)+150*exp(-(t-20).^2/300);
plot3(t,x,y),xlabel('t'),ylabel('DI'),zlabel('APD'),grid
```

Clearly we noticed that the maximum value of DI is 350 msec, at this value the cell is in silent mode for longer time and its firing is at lowest rate, while its minimum value is about 80 msec and at this value the firing of cell is very high. So we can apply two bounds on DI as,

$$80\ msec \leq x(t) \leq 350\ msec \tag{4.5}$$

Similarly we can apply upper and lower limit on APD as,

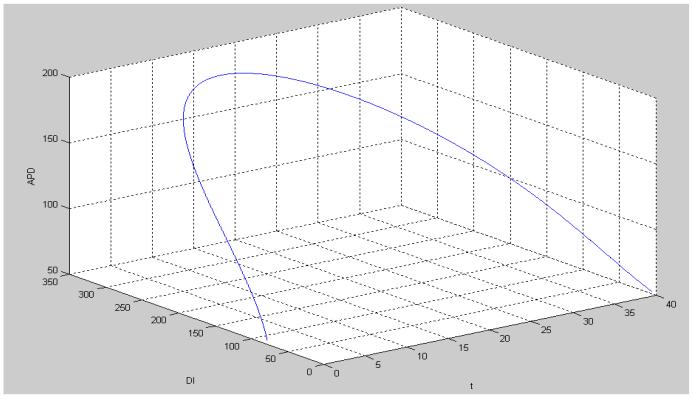

Figure 4.9: 3D plot of APD and DI when $0 \leq t \leq 40msec$

$$50\ msec \leq y(t) \leq 130\ msec \tag{4.6}$$

We can apply biased restitution function depending upon the curve of interest. In this case equations (4.3) and (4.4) can be written as;

$$APD = y(t) = y_o + \alpha e^{-\frac{t-\tau_1}{T_k}} + \beta e^{-\frac{(t-\tau_2)^2}{T_{Na}}} \tag{4.7}$$

$$DI = x(t) = x_o + \gamma e^{-\frac{(t-\tau_3)^2}{T_k}} \tag{4.8}$$

Equations (4.7) and (4.8) are the biased restitution function equations. These equations can be applied whenever the ionic concentration of cell is changed by some external or internal source.

4.4 Refractory Period

The refractory period is the interval of time during which a normal cardiac cell cannot re-excite. The normal refractory period of the ventricle is 250 msec to 300 msec. We can find the upper and lower bound on refractory period by adding equation (4.5) and (4.6);

$$130\ msec \leq RP \leq 480\ msec \tag{4.9}$$

The values in equation (4.9) are very much closer to the actual experimental values.

4.5 Conclusion

Our study is based on the modeling of excitable cells like neurons and cardiac myocytes. We applied the concept of active junctions for the first time and referred such type of junctions as actifiers. Actifiers are electrical circuits that are able to amplify an input signal and have the ability to rectify. We tried to develop a unified model that is capable of simulating both the neuron and the cardiac myocyte. Excitable cells are voltage sensitive structures. A small external voltage that acts as input, can change the dynamics of the cell. We adopted voltage sensitive circuit model in order to capture the dynamics of the excitable cell. Our model is conductance based and its parameters can be easily adjusted. The uniqueness of our model is that we can switch it to cardiac myocyte. By adding a time varying voltage source in series with sodium junction diode we can switch the model for cardiac myocyte. For cardiac myocytes we can implement rhythms that healthy myocyte exhibits as well as arrythmia which is represented by an abnormal myocyte. We suggested the equations for APD (Action Potential Duration) and DI (Diastolic Interval) and found the upper and lower bounds on APD and DI. The findings were found similar to experimental data. We used p-n junction based technique to explain the functioning of channels. This concept of junctions simplified the mathematical modeling of threshold function. Thus, we do not need to use a separate function to describe the thresholds of the cell which reduced our computation cost. Moreover, we used operational amplifier in feedback mode that increases the stability of circuit. The simplicity of the model is compared with other neuron firing models and it is amazing that it only takes 12 flops for neuron and 15 flops for simulating cardiac myocyte. No model for excitable cells have ever proposed that is able to represent the neuron and cardiac myocyte. Our study is the first step to develop a mathematical connection between brain and heart.

Bibliography

[1] AMW Alings, RF Abbas, and LN Bouman. Age-related changes in structure and relative collagen content of the human and feline sinoatrial node a comparative study. *European heart journal*, 16(11):1655–1667, 1995.

[2] Mukund Balasubramanian, Jonathan R. Polimeni, and Eric L. Schwartz. Near-isometric flattening of brain surfaces. *NeuroImage*, 51(2):694 – 703, 2010.

[3] Ben B. Bederson, Richard S. Wallace, and Eric Schwartz. A miniaturized space-variant active vision system: Cortex-I. *Machine Vision and Applications*, 8(2):101–109, 1995.

[4] Benjamin Bederson, Richard Wallace, and Eric L. Schwartz. Cortex-I: A miniaturized space variant active vision system. In Richard J. Mammone, editor, *Artificial Neural Networks for Speech and Vision*. Chapman and Hall, London, 1994.

[5] G. Bonmassar and E. L. Schwartz. Fourier analysis and cortical architectures: the exponential chirp transform. *Real-Time Imaging*, pages 229–237, June 1997.

[6] Patrizia Camelliti, Thomas K Borg, and Peter Kohl. Structural and functional characterisation of cardiac fibroblasts. *Cardiovascular research*, 65(1):40–51, 2005.

[7] Patrizia Camelliti, C Green, and Peter Kohl. *Structural and functional coupling of cardiac myocytes and fibroblasts*, volume 42. Karger Publishers, 2006.

[8] Yi-Hsin Chan, Chia-Tung Wu, Yung-Hsin Yeh, and Chi-Tai Kuo. Reappraisal of luo-rudy dynamic cell model. *Acta Cardiol Sin*, 26:69–80, 2010.

[9] MJ Davies and Ariela Pomerance. Pathology of atrial fibrillation in man. *British heart journal*, 34(5):520, 1972.

[10] MJ Davies and Ariela Pomerance. Quantitative study of ageing changes in the human sinoatrial node and internodal tracts. *British heart journal*, 34(2):150, 1972.

[11] Karima Djabella and Michel Sorine. A Reduced Differential Model of the Electrical Activity of Cardiac Purkinje Fibres. In *28 th Annual International Conference of the IEEE Engineering in Medicine and Biology Society - EMBS'06*, pages 4167–4170, New York, August 2006. IEEE.

[12] Bard Ermentrout. Type i membranes, phase resetting curves, and synchrony. *Neural Comput*, 8:979–1001, 1995.

[13] R. FitzHugh. Impulses and physiological states in theoretical models of nerve membrane. *Biophys. J.*, 1:445–466, 1961.

[14] Giedrius Gaudesius, Michele Miragoli, Stuart P Thomas, and Stephan Rohr. Coupling of cardiac electrical activity over extended distances by fibroblasts of cardiac origin. *Circulation research*, 93(5):421–428, 2003.

[15] Wulfram Gerstner and Werner M. Kistler. Spiking Neuron Models: Single Neurons, Populations, Plasticity. 2002.

[16] Charles M. Gray and David A. Mccormick. Chattering cells: Superficial pyramidal neurons contributing to the generation of synchronous oscillations in the visual cortex. *Science*, 274:109–113, 1996.

[17] R. Grosu, S. Mitra, P. Ye, E. Entcheva, I. V. Ramakrishnan, and S. A. Smolka. Learning cycle-linear hybrid automata for excitable cells. pages 245–258, 2007.

[18] Oliver Hinds, Jonathan R. Polimeni, Niranjini Rajendran, Mukund Balasubramanian, Katrin Amunts, Karl Ziles, Eric L. Schwartz, Bruce Fischl, and Christina Triantafylou. Locating the functional and anatomical boundaries of human primary visual cortex. *NeuroImage*, In Press, 2009.

[19] Oliver P. Hinds, Niranjini Rajendran, Jonathan R. Polimeni, Jean C. Augustinack, Graham Wiggins, Lawrence L. Wald, Diana, Andreas Potthast, Eric L. Schwartz, and Bruce Fischl. Accurate prediction of v1 location from cortical folds in a surface coordinate system. *NeuroImage*, 39(4):1585–1599, February 2008.

[20] A.L. Hodgkin and A.F. Huxley. A quantitative description of membrane current and its application to conduction and excitation in nerve. *Journal of Physiology*, 117:500–544, 1952.

[21] E Izhikevich. Simple model of spiking neurons. *IEEE Trans. Neural Netw*, 14(6):1569–1572, January 2003.

[22] E. M. Izhikevich, N. S. Desai, E. C. Walcott, and F. C. Hoppensteadt. Bursts as a unit of neural information: selective communication via resonance. *Trends in Neurosciences*, 26:161–167, 2003.

[23] Eugene M. Izhikevich. Class 1 neural excitability, conventional synapses, weakly connected networks, and mathematical foundations of pulse-coupled models. *IEEE Transactions on Neural Networks*, 10(3):499–507, 1999.

[24] Eugene M. Izhikevich. Simple model of spiking neurons. *IEEE Transactions on Neural Networks*, 14(6):1569–1572, 2003.

[25] Eugene M. Izhikevich. Which model to use for cortical spiking neurons.pdf:2004 which model to use for cortical spiking neurons.pdf:pdf. *IEEE Transactions on Neural Networks*, 01 2012.

[26] Eugene M. Izhikevich, Joseph A. Gally, and Gerald M. Edelman. Spike-timing dynamics of neuronal groups. *Cerebral Cortex*, 14(8):933–944, August 2004.

[27] Dalane W Kitzman and William D Edwards. Age-related changes in the anatomy of the normal human heart. *Journal of Gerontology*, 45(2):M33–M39, 1990.

[28] Peter Kohl, Patrizia Camelliti, Francis L Burton, and Godfrey L Smith. Electrical coupling of fibroblasts and myocytes: relevance for cardiac propagation. *Journal of electrocardiology*, 38(4):45–50, 2005.

[29] A. Leist, C. J. Scogings, and K. A. Hawick. Simulating anaesthetic effects on a network of spiking neurons with graphics processing units. pages 236–242, 16-19 July 2012.

[30] F. Liu, J. Walmsley, and K. Burrage. Parameter estimation for a phenomenological model of the cardiac action potential. In W. McLean and A. J. Roberts, editors, *Proceedings of the 15th Biennial Computational Techniques and Applications Conference, CTAC-2010*, volume 52 of *ANZIAM J.*, pages C482–C499, July 2011.

[31] P Meyrand, J Simmers, and M Moulins. Dynamic construction of a neural network from multiple pattern generators in the lobster stomatogastric nervous system. *J Neurosci*, 14(2):630–44, February 1994.

[32] Antonio Michelucci, Luigi Padeletti, Giuseppe A Fradella, Raffaele Molino Lova, Domenico Monizzi, Antonio Giomi, and Fabio Fantini. Ageing and atrial electrophysiologic properties in man. *International journal of cardiology*, 5(1):75–81, 1984.

[33] J Müller-Höcker. Cytochrome-c-oxidase deficient cardiomyocytes in the human heart–an age-related phenomenon. a histochemical ultracytochemical study. *The American journal of pathology*, 134(5):1167, 1989.

[34] Kazuki Nakada, Katsumi Tateno, Hatsuo Hayashi, and Kiyonori Yoshii. Functional properties of resonate-and-fire neuron circuits for bio-inspired chemical sensor array. In Akitoshi Hanazawa, Tsutom Miki, and Keiichi Horio, editors, *Brain-Inspired Information Technology*, volume 266 of *Studies in Computational Intelligence*, pages 129–133. Springer, 2010.

[35] Jonathan R. Polimeni, Mukund Balasubramanian, and Eric L. Schwartz. Multi-area visuotopic map complexes in macaque striate and extra-striate cortex. *Vision research*, 46(20):3336–3359, October 2006. Published online July 10, 2006.

[36] Jonathan R. Polimeni, Domhnull Granquist-Fraser, Richard J. Wood, and Eric L. Schwartz. Physical limits to spatial resolution of optical recording: Clarifying the spatial structure of cortical hypercolumns. *Proceedings of the National Academy of Sciences of the United States of America*, 102(11):4158–4163, 15 March 2005.

[37] A. Ramos and E. Schwartz. Observation of frequency specific discharges at the unit level in conditioned cats. *Physiological Behavior*, 16(5):649–652, May 1976.

[38] A. Ramos, E. Schwartz, and E. R. John. Long term recording from cortical and subcortical neurons in unrestrained cats. *Physiological Behavior*, 16(6):803–806, June 1976.

[39] John Rinzel and Bard Ermentrout. Analysis of neural excitability and oscillations. In C. Koch and I. Segev, editors, *Methods in Neuronal Modeling*, chapter 7, pages 251–291. MIT Press, Cambridge, MA, second edition, 1998.

[40] Eric L. Schwartz. Afferent geometry in the primate visual cortex and the generation of neuronal trigger features. *Biological Cybernetics*, 28(1):1–14, 1977.

[41] Eric L. Schwartz. The development of specific visual connections in the monkey and the goldfish: outline of a geometric theory of receptotopic structure. *Journal of Theoretical Biology*, 69(4):655–683, 1977.

[42] Eric L. Schwartz. Computational anatomy and functional architecture of striate cortex: a spatial mapping approach to perceptual coding. *Vision Research*, 20(8):645–669, 1980.

[43] Eric L. Schwartz. A quantitative model of the functional architecture of human striate cortex with application to visual illusion and cortical texture analysis. *Biological Cybernetics*, 37(2):63–76, 1980.

[44] Eric L. Schwartz. Cortical anatomy, size invariance, and spatial frequency analysis. *Perception*, 10(4):455–468, 1981.

[45] Eric L. Schwartz, A. Ramos, and E. Roy John. Cluster analysis of evoked potentials from behaving cats. *Behavioral Biology*, 17(1):109–117, May 1976.

[46] Isao Shiraishi, Tetsuro Takamatsu, T Minamikawa, Z Onouchi, S Fujita, et al. Quantitative histological analysis of the human sinoatrial node during growth and aging. *Circulation*, 85(6):2176–2184, 1992.

[47] D. Tal and E. L. Schwartz. Topological singularities in cortical orientation maps: the sign theorem correctly predicts orientation column patterns in primate striate cortex. *Network: Computation in Neural Systems*, 8(2):229–238, May 1997.

[48] Doron Tal and Eric L. Schwartz. Weber-Fechner transduction: a logarithmic compressive nonlinearity is a generic property of integrate and fire neurons. In *World Congress on Neural Networks-San Diego. 1994 International Neural Network Society Annual Meeting*, volume 4 of *Proceedings of World Congress on Neural Networks*, pages 360–367, Hillsdale, NJ, June 5–9 1994. International Neural Network Society, Lawrence Erlbaum Associates.

[49] Doron Tal and Eric L. Schwartz. Computing with the leaky integrate-and-fire neuron: Logarithmic computation and multiplication. *Neural Computation*, 9(2):305–318, Feb. 15 1997.

[50] Claude Thery, Bernard Gosselin, Jean Lekieffre, and Henri Warembourg. Pathology of sinoatrial node. correlations with electrocardiographic findings in 111 patients. *American heart journal*, 93(6):735–740, 1977.

[51] F. J. Varela, A. Toro, E. R. John, and E. L. Schwartz. Perceptual framing and cortical alpha rhythm. *Neuropsychologia*, 19(5):675–686, 1981.

[52] T. Verechtchaguina, I. M. Sokolov, and Lutz Schimansky-Geier. Interspike interval densities of resonate and fire neurons. *Biosystems*, 89(1-3):63–68, 2007.

[53] Chong Wang, Peter Beyerlein, Heike Pospisil, Antje Krause, Chris Nugent, and Werner Dubitzky. An efficient method for modeling kinetic behavior of channel proteins in cardiomyocytes. *IEEE/ACM Transactions on Computational Biology and Bioinformatics*, 9(1):40–51, 2012.

[54] R. J. Wood and E. L. Schwartz. Topographic shear and the relation of ocular dominance columns to orientation columns in primate and cat visual cortex. *Neural Networks*, 12(2):205–210, March 1999.

[55] Y. Yeshurun and E. L. Schwartz. Cortical hypercolumn size determines stereo fusion limits. *Biological Cybernetics*, 80(2):117–129, February 1999.

[56] Frank CP Yin, Harold A Spurgeon, HL Greene, Edward G Lakatta, and Myron L Weisfeldt. Age-associated decrease in heart rate response to isoproterenol in dogs. *Mechanisms of ageing and development*, 10(1):17–25, 1979.